ANL-7560

ANL-7560

Argonne National Laboratory

FAULT PROPAGATION IN AN EBR-II MARK-II DRIVER-FUEL SUBASSEMBLY

by

A. V. Campise

DISCLAIMER

The facilities of Argonne National Laboratory are owned by the United States Government. Under the terms of a contract (W-31-109-Eng-38) between the U. S. Atomic Energy Commission, Argonne Universities Association and The University of Chicago, the University employs the staff and operates the Laboratory in accordance with policies and programs formulated, approved and reviewed by the Association.

MEMBERS OF ARGONNE UNIVERSITIES ASSOCIATION

The University of Arizona	Kansas State University	The Ohio State University
Carnegie-Mellon University	The University of Kansas	Ohio University
Case Western Reserve University	Loyola University	The Pennsylvania State University
The University of Chicago	Marquette University	Purdue University
University of Cincinnati	Michigan State University	Saint Louis University
Illinois Institute of Technology	The University of Michigan	Southern Illinois University
University of Illinois	University of Minnesota	University of Texas
Indiana University	University of Missouri	Washington University
Iowa State University	Northwestern University	Wayne State University
The University of Iowa	University of Notre Dame	The University of Wisconsin

Printed in the United States of America
Available from
Clearinghouse for Federal Scientific and Technical Information
National Bureau of Standards, U. S. Department of Commerce
Springfield, Virginia 22151
Price: Printed Copy $3.00; Microfiche $0.65

ANL-7560
Reactor Technology

ARGONNE NATIONAL LABORATORY
9700 South Cass Avenue
Argonne, Illinois 60439

FAULT PROPAGATION IN AN EBR-II MARK-II DRIVER-FUEL SUBASSEMBLY

by

A. V. Campise

EBR-II Project

March 1969

THIS PAGE

WAS INTENTIONALLY

LEFT BLANK

TABLE OF CONTENTS

LIST OF FIGURES

LIST OF FIGURES

LIST OF FIGURES

LIST OF TABLES

NOMENCLATURE

A	Cross-sectional area, $in.^2$
A_f	Area of interstitial flow channel, $in.^2$
A_R	Area of rupture hole, $in.^2$
A_0	Area of flow path upstream from rupture hole, $in.^2$
A_2	Area of exit sodium coolant stream, $in.^2$
B/U	Fuel burnup, MWd/MT
C	Discharge coefficient
C_p	Specific heat at constant pressure, cal/g-°C
C_v	Specific heat at constant volume, cal/g-°C
D	Inside diameter of rupture hole, ft
D_{eff}	Effective circular diameter of rupture hole, in.
D.R.	Gas discharge rate, $in.^3/sec$
E_f	Energy content in fuel, J/g of fuel
E_p	Specific plastic energy, $in.\text{-}lb/in.^3$
E_p^{ss}	Specific plastic energy for stainless steel, in.-lb/lb
E_{RE}	Radial damage component of energy release, in.-lb
E_T	Total energy released from an interaction of sodium and molten fuel, in.-lb
F_B	Weight rate of flow of sodium bond from rupture hole, lb/sec
g_c	Conversion factor, 32.17 ft-lb/lb(force)-sec^2
g_L	Local acceleration due to gravity, ft/sec^2
ΔH	Distance from top of fuel pin, in.
k	Ratio of specific heats of fission gas, C_p/C_v
L	Latent heat of evaporation of sodium, J/g
m	Mass of liquid sodium, g/g of fuel
m_0	Initial mass of fission gas, lb
m_1	Transient mass of fission gas, lb
$(m_1)_c$	Mass of fission gas at critical pressure ratio for sonic flow, lb
m_2	Total mass of fission gas released, lb
MT	Metric ton
MWd	Megawatt days
P_{cr}	Critical pressure ratio for fission gas; the point at which sonic flow develops through perforation in cladding
P_V	Vapor pressure of sodium, $dynes/cm^2$
P_0	Internal fission-gas pressure due to irradiation, psi
P_1	Transient pressure, psi
P_2	External system pressure, psi
R	Universal gas constant, ft-lb/lb-°R
S_f	Specific heat of liquid fuel, J/g-°C
S_{gp}	Specific heat of sodium at constant pressure, J/g-°C
S_{gv}	Specific heat of sodium vapor at constant volume, J/g-°C
S_ℓ	Specific heat of liquid sodium, J/g-°C
T	Absolute temperature, °K
T_c	Temperature of liquid sodium, °K
T_f	Temperature of liquid fuel, °K
T_V	Temperature at which all available sodium is vaporized, °K
T_0	Internal temperature of fission gas, °F
T_1	Transient temperature, °F
T_2	System temperature, °F
$\Delta T/\Delta P$	$\frac{\text{Change in temperature, °C}}{\text{Change in pressure, atm}}$
t_B	Time a channel is blocked, sec
t_c	Time at critical gas flow, sec
V	Flow velocity of sodium bond through rupture hole, ft/sec
V_c	Volume of gas available, $in.^3$
V_f	Volume of fuel melted, $in.^3$
V_{STP}	Volume of fission gas at standard temperature and pressure, ft^3
V_0	Internal fission-gas volume due to irradiation, $in.^3$
V_1	Transient volume, $in.^3$
V_2	System volume, $in.^3$
$\Delta V/V$	% change in fuel volume
V_f	Local coolant flow velocity, $in.^3/sec$
W	Work, J
W_{FP}	Weight of fission gas, lb
W_{max}	Maximum work from interaction of sodium and molten fuel, J/g of fuel
W_{ss}	Weight of stainless steel, lb
W_T	Total energy release from interaction of sodium and molten fuel, J/g of fuel involved
W_1	Additional work, J/g of fuel
x	Mass of sodium vapor, g/g of fuel
Z_0	Initial height of sodium bond, ft
Z_1	Distance from bottom of fuel element to rupture hole, ft
α	Ratio of cross-sectional area of rupture hole to inside-diameter area of cladding
ϵ_p	Total strain
σ	Tensile strength, psi
σ_d	Dynamic tensile-yield strength, psi
ρ	Density, lb/ft^3
ρ_{Na}	Sodium density, lb/ft^3
μ	Viscosity of sodium bond, lb/sec-ft
ω	Weight rate of flow of fission gas, lb/sec

FAULT PROPAGATION IN AN EBR-II MARK-II DRIVER-FUEL SUBASSEMBLY

by

A. V. Campise

ABSTRACT

The consequences of cladding failures in a Mark-II EBR-II experimental fuel element were evaluated under steady-state power. The principal consequences considered were the blanketing of adjacent fuel elements in a fuel subassembly with fission gas and the interactions of sodium and molten fuel following a partial loss of sodium bond in a fuel element. The possibility of fault propagation was evaluated based on physical properties of the Mark-II driver-fuel subassembly and the EBR-II reactor core. The results indicate an extremely low probability for propagation of faults in fuel elements due to gas blanketing or rapid formation of sodium vapor resulting from interaction of sodium and molten fuel. Upper-limit conditions for fault propagation are shown to be restricted to an area of thermohydrodynamic combined-system values that indicate an extremely low probability of occurrence.

I. INTRODUCTION

The principal objective[1] of the EBR-II Mark-II fuel-development program is the successful design of a metallic driver-fuel system capable of irradiation exposures of 2 a/o or greater at the reactor's design power level of 62.5 MWt. As an intermediate step in the fuel-development program, five driver-fuel subassemblies, each containing 91 unencapsulated Mark-II elements, will be fabricated and irradiated in the EBR-II core. The required safety analysis for the experimental irradiation of these subassemblies prompted this study of fault* propagation in a Mark-II driver-fuel subassembly. Although the principal models used in this study are applied only to the Mark-II driver fuel, the results of the study are sufficiently generalized to be applicable to the present Mark-IA fuel at slightly different operating conditions. The Mark-II and -IA fuel elements are similar in concept.

---

*Fault: A flaw or defect in the structure of a fuel element that leads to local abnormal operating conditions.

Emphasis in fast-reactor safety is being placed on attaining a basic understanding of various modes of propagating faults in fuel elements. Because of its safety implications, fault propagation in the cores of large fast breeder reactors will be given an increased amount of analytical and experimental attention. The entire area of fault propagation is too large to cover in one report; therefore, the scope of this report has been limited to steady-state fault conditions. Other failure modes, such as nuclear and loss-of-flow transients, could cause propagation of faults in Mark-II subassemblies. These transient conditions are not considered in this report, which primarily covers credible failures of fuel elements under steady-state power operation and the possible consequences that may follow these initial failures. Nuclear transients and loss-of-flow accidents will be the subject of a preliminary safety-analysis report on the Mark-II core loading for EBR-II.

The possibility of propagation of faults in EBR-II Mark-II driver-fuel elements is of prime concern to the safe operation of the EBR-II as an irradiation facility. To date, only a few statistical data points are available that are directly applicable to faults in Mark-II fuel elements at steady-state conditions.[2] An increased experimental effort is required in this area to enlarge our understanding of the various fault paths that an initial failure may follow.

The principal failure mechanisms and consequences considered for the EBR-II Mark-II driver-fuel element are those initiated by a cladding failure that is followed by a loss of sodium bond, melting of fuel, interaction of sodium and molten fuel, and finally, release of fission gas. The cause of the initial cladding failure is not discussed in this report. The consequences of this failure are evaluated under varying fuel-element and reactor operating conditions.

Although fault propagation could be more critical in ceramic-fueled experiments (owing to the reduced thermal conductivity and higher operating temperatures), only EBR-II Mark-II metallic driver fuel is considered. The principal investigation discussed in this report is directed at the hottest single fuel element in a subassembly and the influence of an initial fault in this element on adjacent fuel elements in the subassembly. Propagation of a fault to surrounding subassemblies is briefly considered in Section IV.B.

The primary approach adopted in this report is to establish the conditions under which fuel-element fault propagation can occur and to identify the upper-limit values for the worst case, using known physical principles.

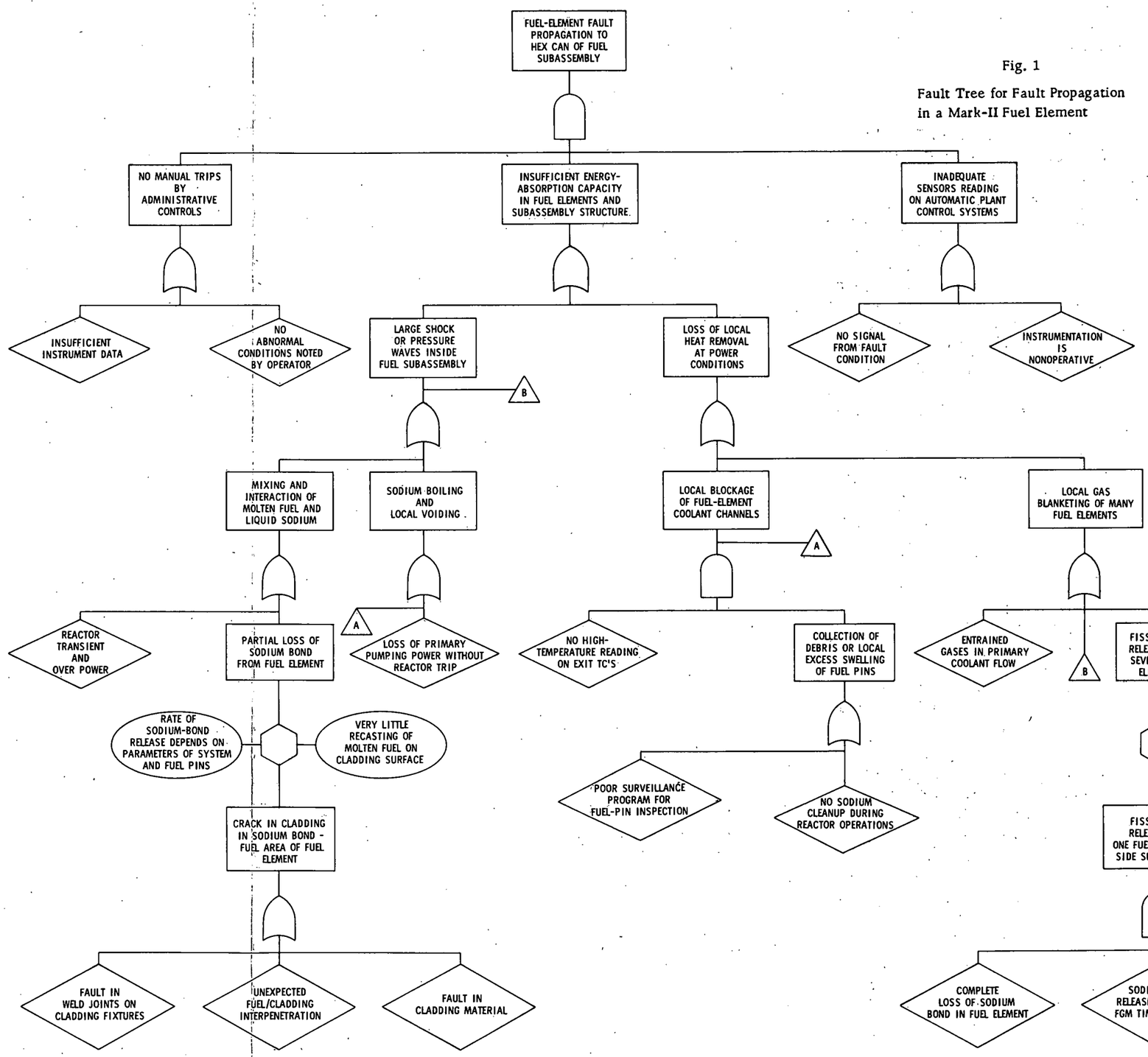

Fig. 1

Fault Tree for Fault Propagation in a Mark-II Fuel Element

II. FAULT-PROPAGATION MODES

A. Fault-tree Analysis

The principal modes of fault propagation from a failed EBR-II Mark-II fuel element are: (1) mixing and interaction of molten fuel and liquid sodium; (2) boiling of sodium and local voiding; (3) local blockage of coolant channels in fuel elements; and (4) local blanketing of many fuel elements with gas. Fault-tree analysis[3] has been used to develop an overview of the causes of these modes of propagation and the consequences following their occurrence. Figure 1 shows a fault tree with an identified, undesirable end point of the propagation of an element fault to the hexagonal can of the Mark-II subassembly. Several branches of this tree are identified, including the modes of propagation listed above. (The body of this report is directed toward those branches of the tree involving the mixing and interaction of molten fuel and liquid sodium and the local blanketing of fuel elements with gas.) Figure 2 explains the symbols used in the fault tree. The triangular symbol shown in Fig. 2 is used as a shorthand method of indicating position of duplicate tree branches that are shown elsewhere in the fault tree. For example, all branches of the tree shown under the uppermost triangle containing a B (near the top of Fig. 1) also should be considered as placed at the lower triangle containing a B. The two triangles containing A's serve a similar purpose in Fig. 1.

The following is a brief explanation of the two branches of the illustrated fault tree that will be emphasized in this report.

1. Interaction of Liquid Sodium and Molten Fuel

This branch of the tree could be initiated by any of the following: (a) a fault in the weld joints of the end pieces of cladding; (b) an unexpected fuel-cladding interpenetration and cladding failure; or (c) a fault in the cladding material.

Any of these events could lead to a break in the cladding, and this break is assumed to occur in the sodium-bonded fuel region of the element. The amount of subsequent loss of sodium bond from the element depends on the rate of release of sodium bond and the parameters of the reactor system and fuel element (e.g., the size of the hole, the internal pressure, the burnup on the pins). It is assumed, in this branch of the fault tree, that very little molten fuel is recast on the cladding surface while the sodium is released.

The above events lead to a partial loss of sodium bond from the element. This loss, in turn, leads to conditions under which molten fuel (formed from unbonding of the fuel while the reactor is still at steady-state conditions) can now mix with the liquid sodium bond remaining in the fuel

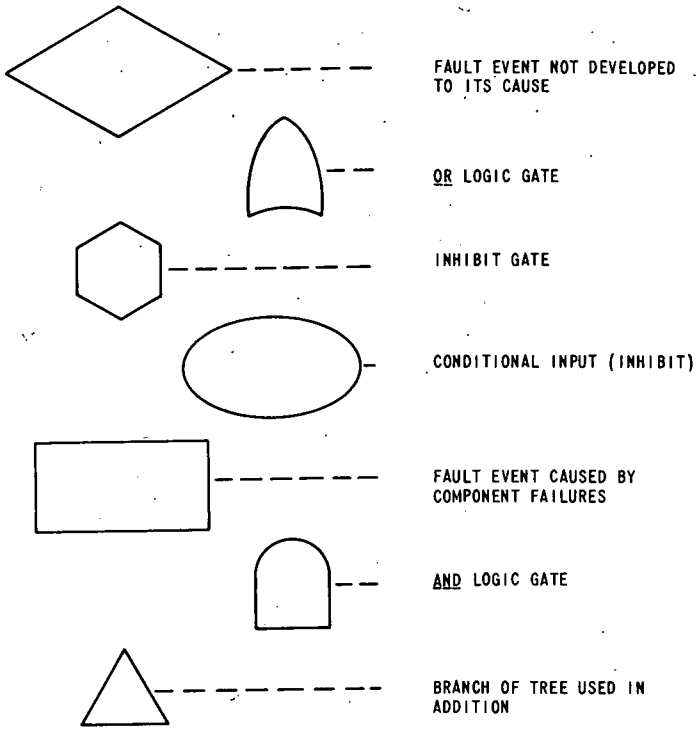

Fig. 2
Fault-tree Symbols

element. As a further consequence, a shock or pressure wave can be generated inside the subassembly because of the formation of sodium vapor in the fuel element. If we assume, for a moment, that there is insufficient energy-absorption capability in the fuel elements and the subassembly structure, this mixing of molten fuel and liquid sodium can lead to propagation of a fuel-element fault to the hexagonal can of the fuel subassembly. A similar consequence can occur with local gas blanketing of fuel elements with gas.

2. Local Gas Blanketing of Fuel Elements

For this branch of the fault tree, conditions assumed to exist were: (a) complete loss of sodium bond in the fuel element; (b) loss of the sodium bond too rapidly for the fission gas monitor (FGM) to respond; and (c) no signal from the fuel-element rupture detector (FERD) loop in the EBR-II system.

Under these conditions, fission gas is assumed to be released from one fuel element in a subassembly. The consequences of this fission-gas release depend on the parameters of the reactor system and the element (e.g., internal pressure, burnup on the fuel, size of the ruptured hole, external system pressures). Assuming gas blanketing and failure of adjacent fuel elements, fission gas can then be released from several elements because of this gas blanketing. This released fission gas blankets additional fuel elements, causing additional gas to be released and increasing the operating temperature of more fuel elements. This leads to

a local loss of heat-removal capability at reactor power conditions. If this fault is allowed to continue, there would be insufficient energy-absorption capability in the fuel elements and subassembly structure; thus, overheating would occur, and the fault would be propagated to the entire subassembly.

Other branches of the fault tree are presented in Fig. 1 for completeness and are self-explanatory. The top part of the tree indicates the action of the plant control system that allows the fault to propagate to a point at which the hexagonal can of the fuel subassembly is involved.

In summary, the above fault-tree analysis was used to establish the sequence of events and conditions following the initial penetration of the cladding of a fuel element and the conditions required for propagating the fault to adjacent fuel elements and the subassembly structure. A fault tree provides a display of various groupings of possible faults and conditions which can lead to an undesirable consequence. The prime merit of a fault-tree approach is that it provides a measurement of the inherent safety in the system and is a distinct aid in the evaluation of the overall impact of the fault to the system. Displayed in the fault tree are the sequence of events, the system response to these events, and the conditions under which the events continue to the point where the undesirable consequence must be evaluated.

B. Configurations of Initial Faults in Fuel Elements

Figure 3 shows the arrangement of fuel elements in a Mark-II subassembly. In this subassembly, three conditions of fuel-element faults, events, and propagation modes are considered:

1. Loss of sodium bond and possible interaction of sodium and molten fuel (depicted in Fig. 4). It is assumed that a break occurred at the bottom of the fuel element, and, depending on system conditions and the operating conditions of the fuel elements, the sodium bond is released from the element.

2. Release of fission gas and gas blanketing of adjacent fuel elements (depicted in Fig. 5). It is assumed that the sodium bond is lost from the element and that the fission gas is released from the bottom of the element (considered to be the worst case). Figure 5 shows the triangular pitch of the fuel elements in an EBR-II Mark-II subassembly and the interstitial regions that will be studied for the effect of blanketing by fission gas.

3. Combined effects of 1 and 2 at "beginning" and "end-of-life" conditions in the Mark-II fuel element (depicted in Fig. 6). In the beginning-of-life condition, the fuel elements are shown with a sodium bond around the fuel pin. At the end-of-life condition, the sodium bond is greatly reduced around the fuel pin because the Mark-II fuel element is designed to expand

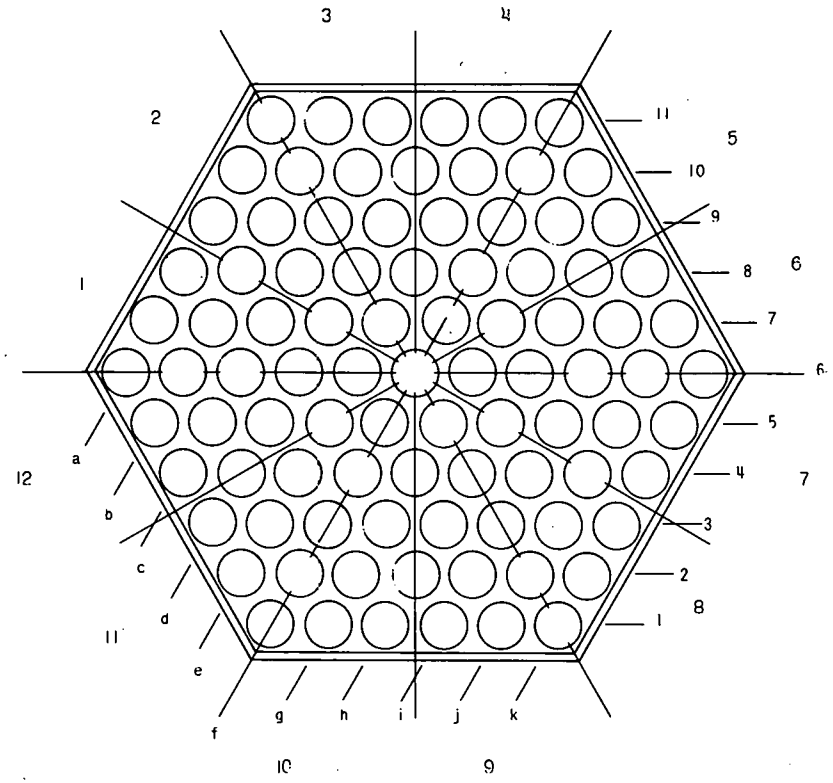

Fig. 3. Arrangement of Fuel Elements in a Mark-II Subassembly

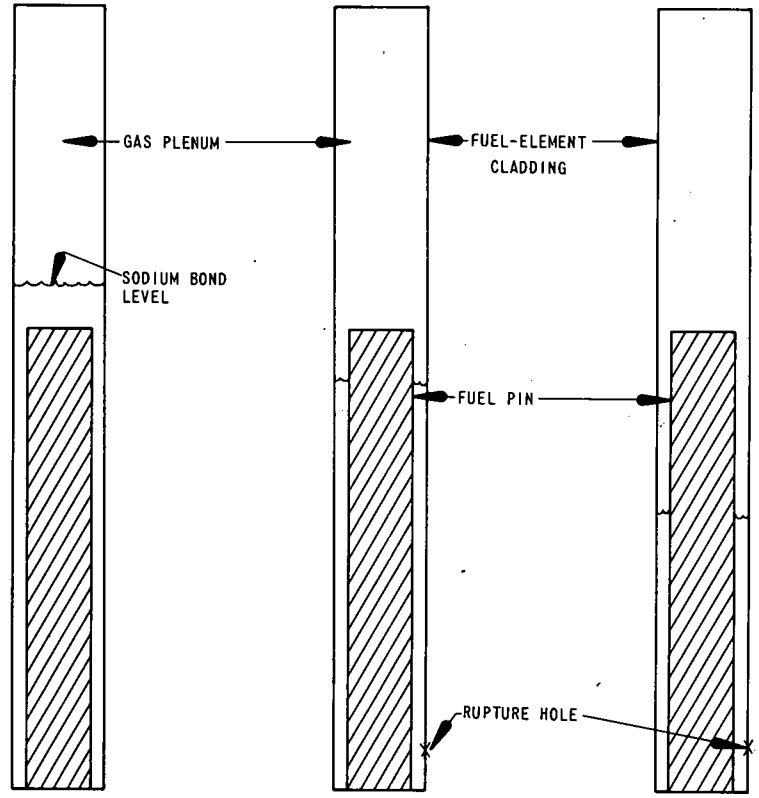

Fig. 4. Configuration for Release of Sodium Bond and Interaction of Sodium and Molten Fuel

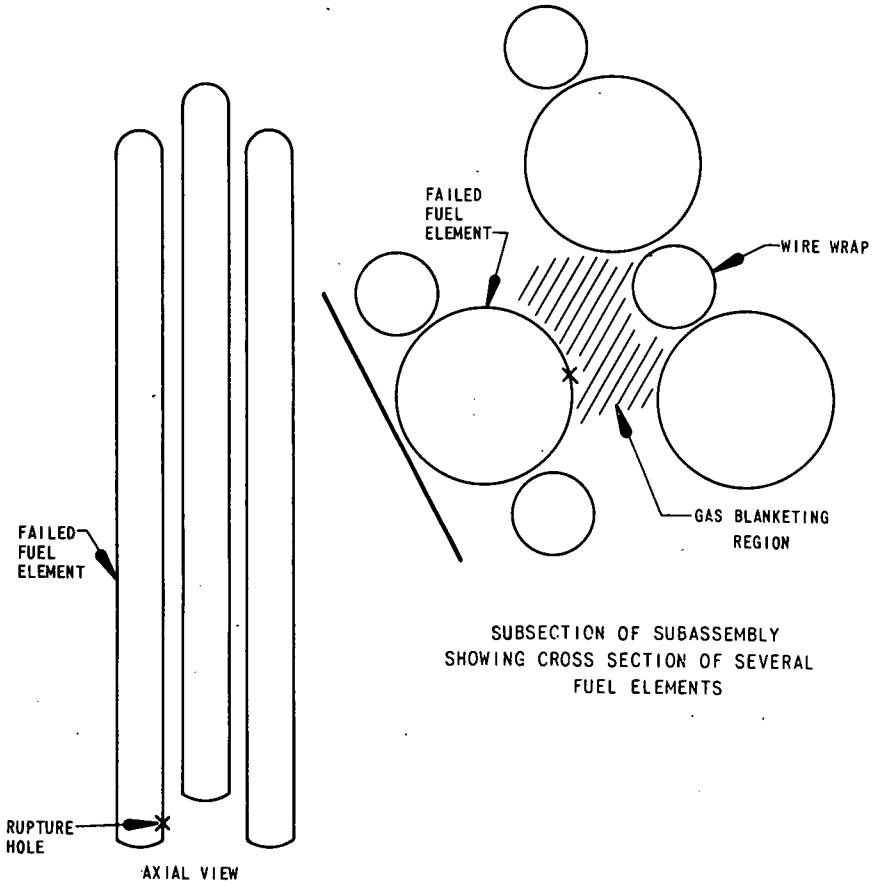

Fig. 5. Configuration for Release of Fission Gas and Gas Blanketing

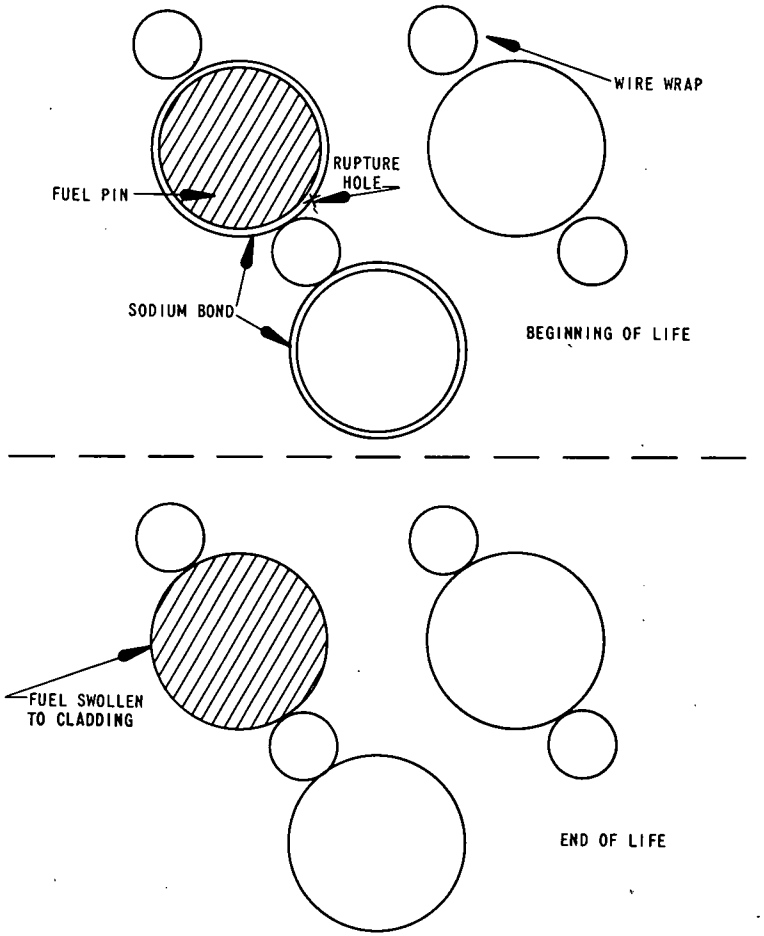

Fig. 6. Combined Effects at Beginning- and End-of-life Conditions in Fuel Elements

and contact the cladding.[1] The latter condition is studied to evaluate the effects of the large reduction of sodium bond on material temperatures.

These three basic configurations will be referred to in this report.

III. KINETIC STUDIES

A. Models

Several theoretical models[4] were used to simulate the following conditions: (1) release of sodium bond; (2) release of fission gas; (3) interactions of sodium and fuel; (4) material temperatures resulting from gas blanketing; and (5) temperatures and volume of fuel melted during loss of sodium bond. Assumptions and limitations of the first three theoretical models are given in detail in the appendixes. Figures 7-11 are graphic representations of all five models along with the important variables considered.

Figure 7 shows the model for release of sodium bond. As indicated, principal variables to consider are:

P_0, the internal fission-gas pressure due to irradiation;

P_2, the external system pressure;

A_R, the area of the rupture hole;

Z_0, the initial height of the sodium bond;

Z_1, the distance from the bottom of the fuel element to the rupture hole; and

ρ_{Na}, is the density of sodium.

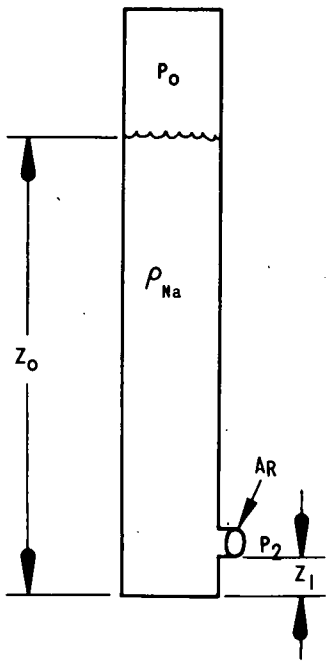

Fig. 7
Model for Release of Sodium Bond

Figure 8 shows the model depicting release of fission gas. The principal variables in this model are:

P_0, the internal fission-gas pressure due to irradiation;

T_0, the internal temperature of the fission gas;

$k = C_p/C_v$, the ratio of specific heats of the fission gas;

P_{cr}, the critical pressure ratio for the fission gas;

A_R, the area of the rupture hole;

P_2, the external system pressure; and

MWd/MT, the fuel burnup.

These are principal variables governing release of fission gas. The conditions leading up to P_0 are discussed in detail in Appendix B.

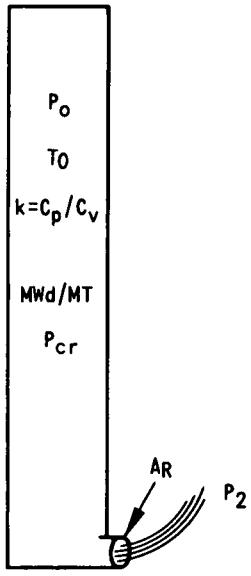

Fig. 8

Model for Release of Fission Gas

Figure 9 shows the model for interaction of sodium and molten fuel. The principal variables in this model[5] are:

T_f, the temperature of liquid fuel;

T_c, the temperature of liquid sodium;

S_f, the specific heat of the liquid fuel;

S_l, the specific heat of the liquid sodium;

S_{gp}, the specific heat of sodium at constant pressure;

L, the latent heat of evaporation of sodium; and

V_f, the volume of fuel melted.

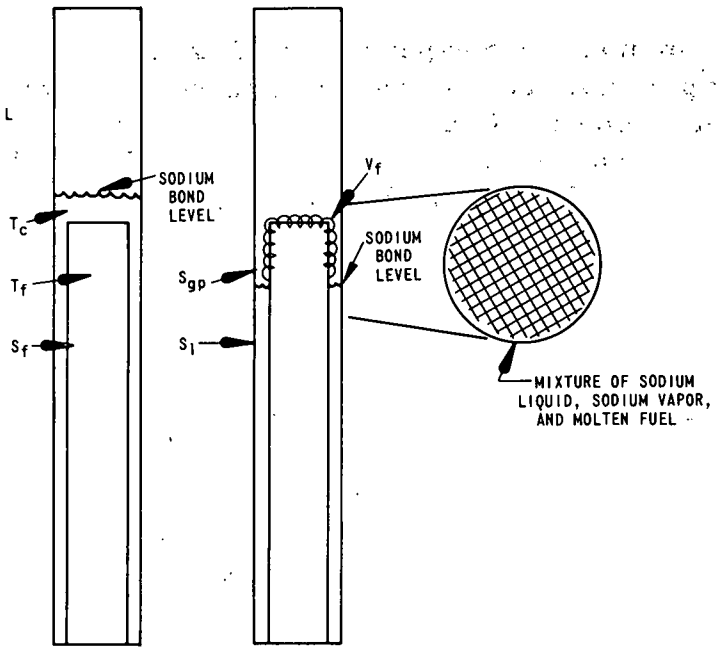

Fig. 9

Model for Interaction of Sodium and Molten Fuel

Figure 10 shows the heat-transfer model used to compute the material temperatures following gas blanketing of various sectors around a Mark-II fuel element. The principal variable in this study was the sector of the cladding surface blanketed with fission gas. The hottest element was assumed to be located in Row 4 or 5 of the EBR-II core, and the reactor was assumed to be operating at 50 or 62.5 MWt.

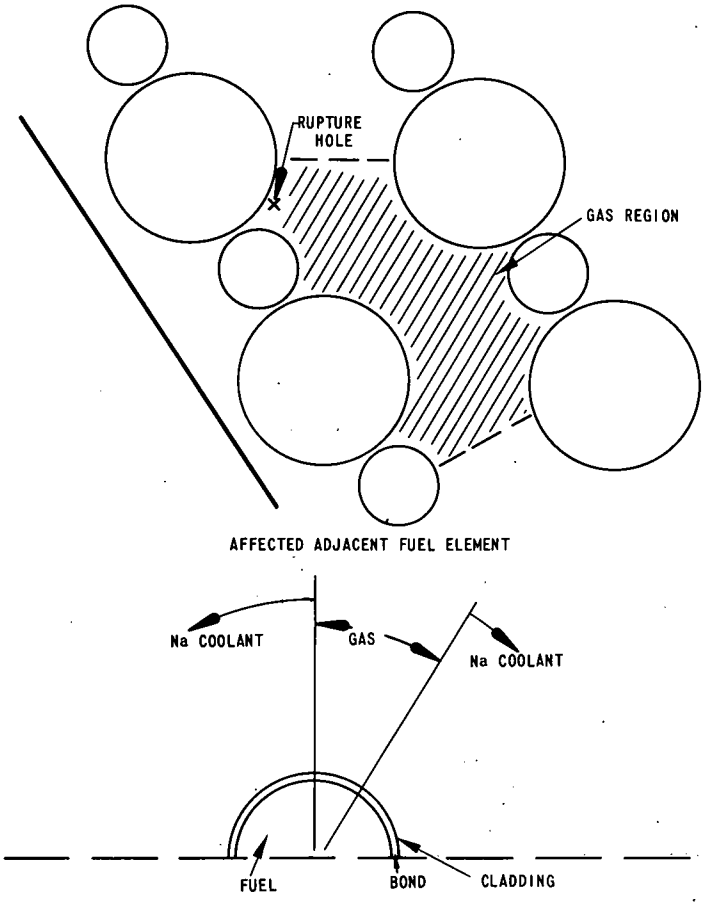

Fig. 10. Gas-blanketing Model Used to Compute Material Temperatures

Figure 11 was used to compute material temperatures following the loss of sodium bond. In this axial view of the fuel element, the top part of the pin is bonded with fission gas and the remainder of the fuel pin is bonded with sodium.

B. Assumed Operating Conditions for Mark-II Fuel Elements

Table I compares the physical dimensions and properties of the Mark-II fuel elements[1] to present and past designs. The following studies of fault propagation assume that the amount of fission-gas release is properly

bracketed on the lower end by measured experimental data (as shown in Fig. 12) and that, on the upper end, 100% of the gas produced is released to the plenum within the fuel element. In addition, the burnup on the Mark-II fuel element will be assumed to vary from 0 to 5 a/o. Finally, reactor power levels of 50 and 62.5 MWt will be considered.

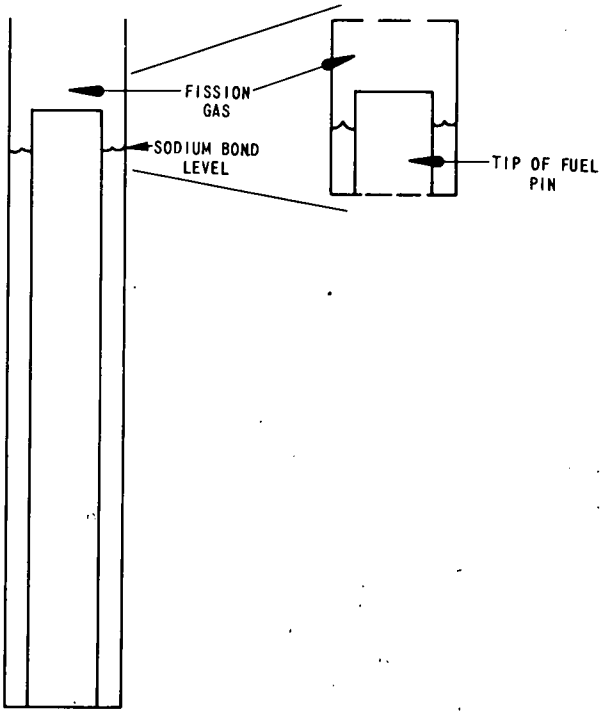

Fig. 11

Axial Model Used to Compute Material Temperatures Following Loss of Sodium Bond

TABLE I. Design Features of EBR-II Fuel Elements

	Type of Fuel Element			
	I	IA	IB	II
Cladding OD, in.	0.174	0.174	0.174	0.174
Cladding ID, in.	0.156	0.156	0.156	0.150
Cladding thickness, in.	0.009	0.009	0.009	0.012
Sodium-annulus thickness, in.	0.006	0.006	0.006	0.010
Fuel-pin diameter, in.	0.144	0.144	0.144	0.130
Fuel-pin length, in.	14.2	13.5	13.5	14.2
Fuel-pin mass, g	67.6	64.3	64.3	54.5
Element length, in.	18	18	18	26
Effective fuel density, %	85	85	85	75
Fuel-pin-restrainer gap, in.	0.40	0.40	0.40	a
(Vol plenum/Vol fuel) x 100	13.2	18.5	25.8	99
Number of fuel elements per subassembly	91	91	91	91

[a]Not selected at time of writing.

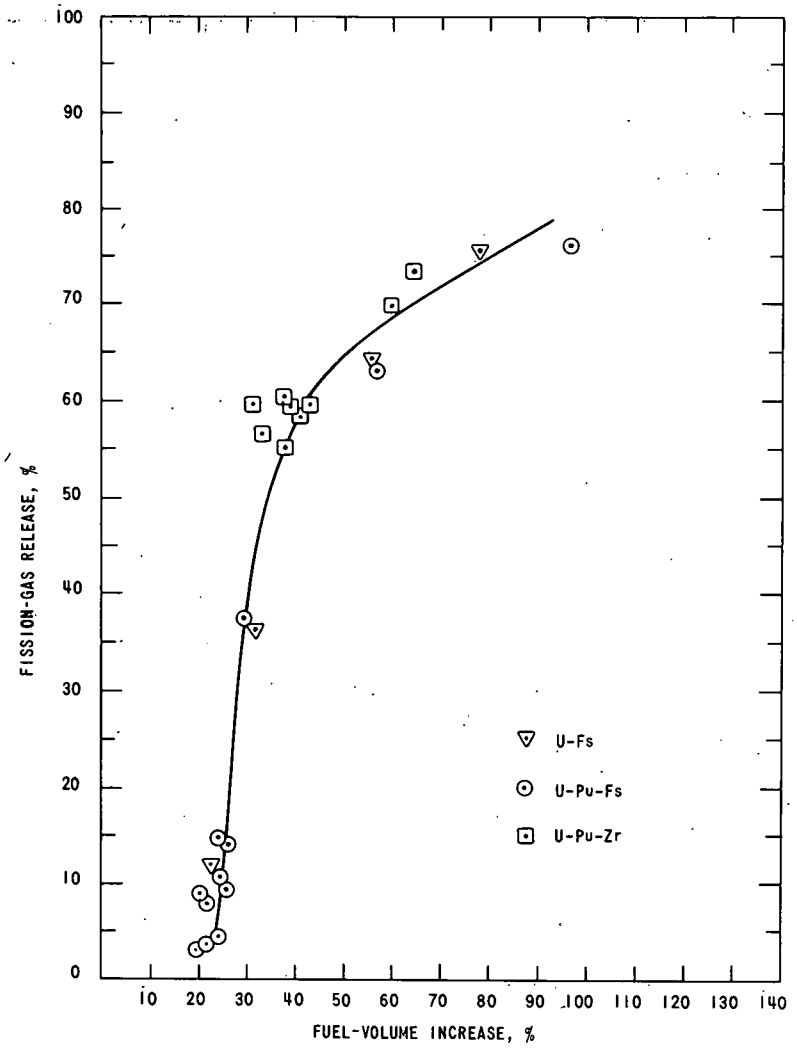

Fig. 12. Measured Release of Fission Gas as Fuel Swells

Figure 13 shows the approximately linear rate of swelling vs burnup for Mark-LA fuel. In the present study, the relationship between swelling rates and burnup in the Mark-II pins was assumed to be linear (as plotted in Fig. 14). This assumption allows us to convert fission-gas release vs swelling to fission-gas release vs burnup. Figure 15 shows the results of this conversion. This figure will be referred to in the text as "experimental data" and will be used as the lower limit of the fission-gas release. The upper limit, as mentioned above, will be assumed to be 100% fission-gas release.

C. Release of Sodium Bond

The release of sodium bond from the Mark-II fuel element depends on the initial internal gas pressure, the location of the rupture hole and its area, and the external system pressure. In computing the rate of

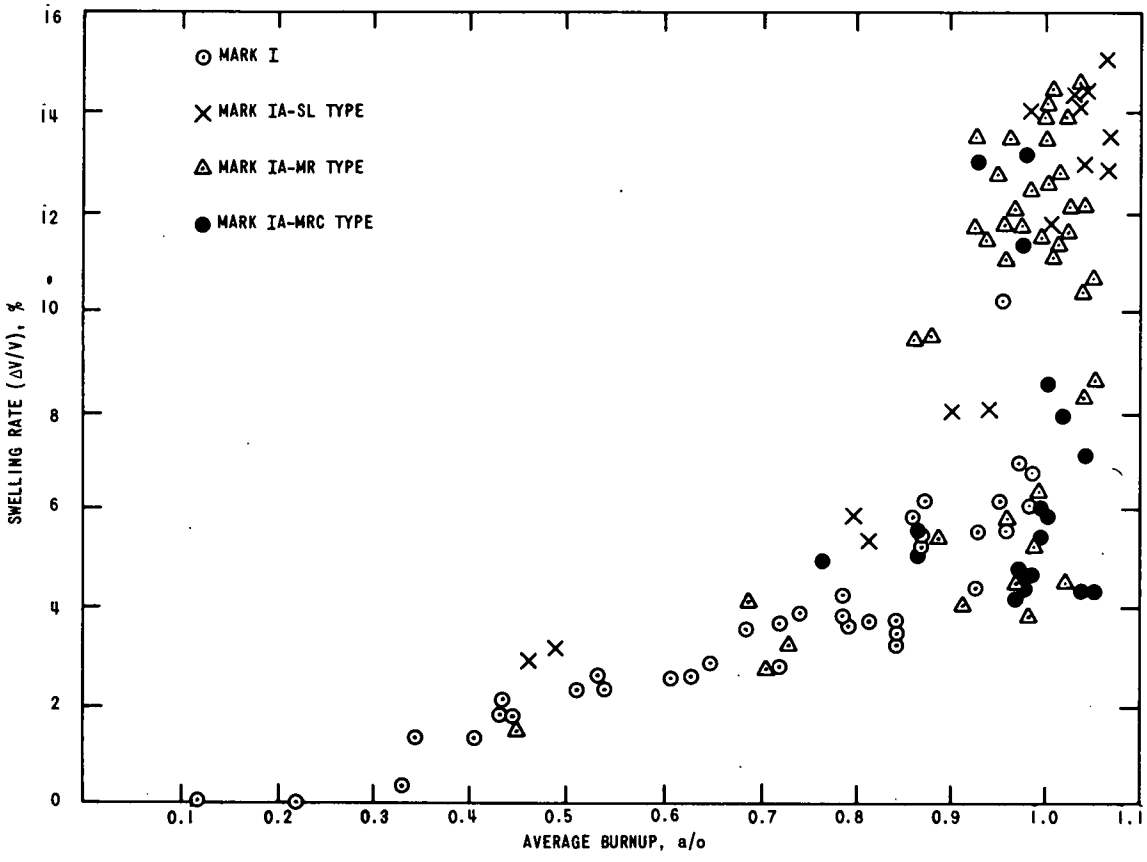

Fig. 13. Measured Swelling Rate of Mark-I and -IA Fuels, as a Function of Burnup

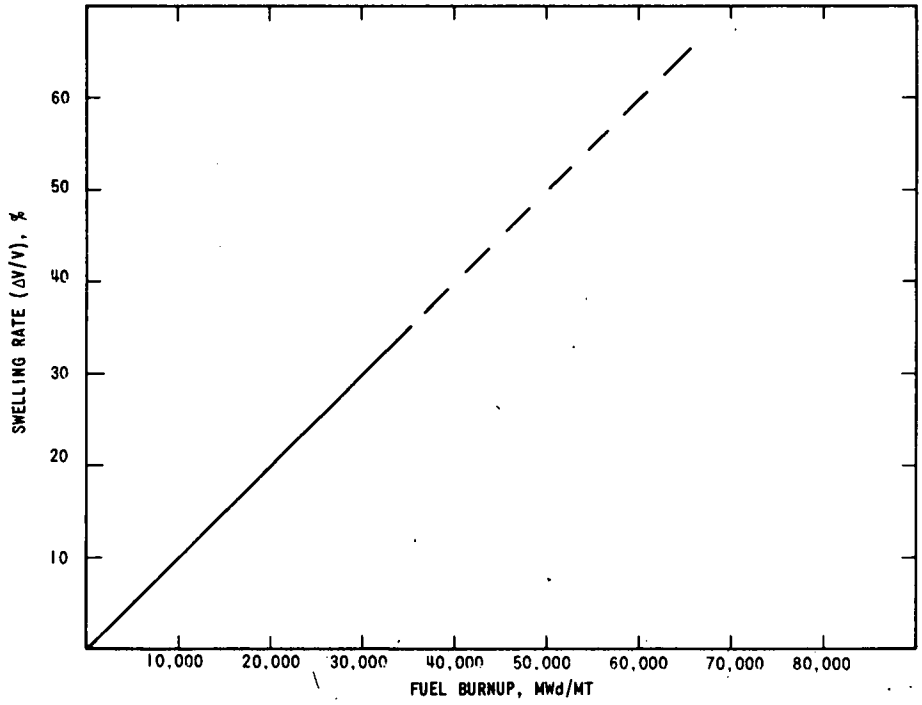

Fig. 14. Assumed Swelling Rate of Mark-II Fuel, as a Function of Burnup

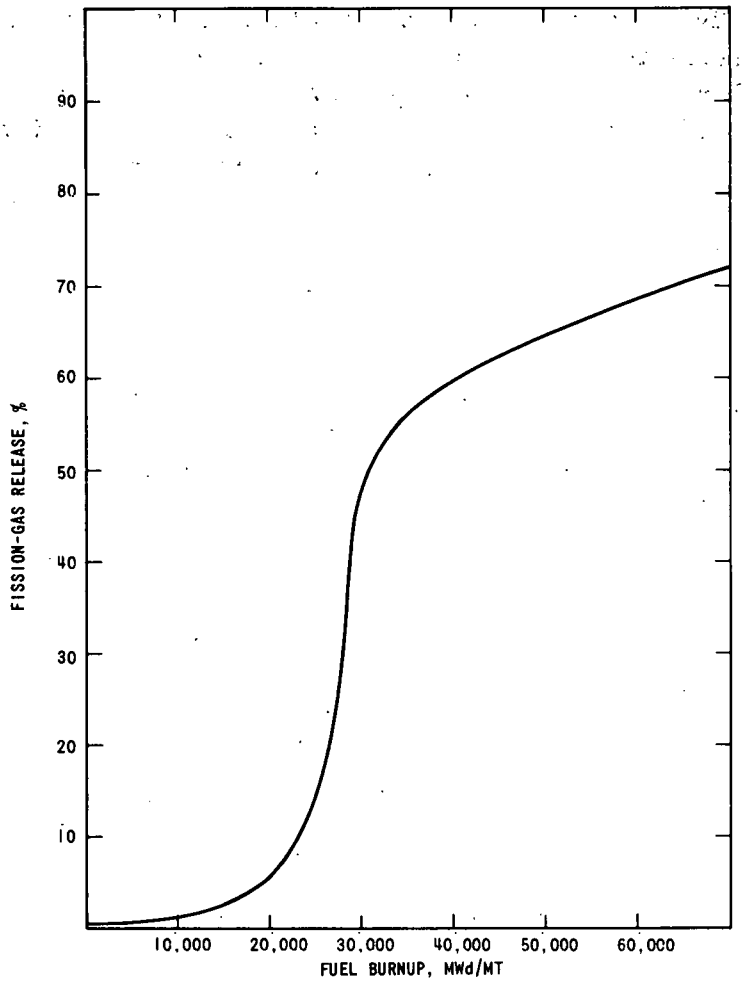

Fig. 15. Assumed Fission-gas Release from a Mark-II Fuel Element, as a Function of Burnup

sodium-bond release, we assumed that the characteristics of the rate of flow of sodium through the hole were similar to the characteristics of the rate of flow of liquid through an orifice. Hole sizes with effective circular diameters of 1-20 mils were studied. (The reason for choosing this range of hole sizes will be explained in Section III.D. These values are considered to be the upper and lower limits of hole sizes that could cause the right conditions for Mark-II fault propagation.) Figure 16 shows the time required to expel sodium bond from a Mark-II fuel element, as a function of fuel burnup and effective circular diameter of rupture hole (D_{eff}). The figure also shows the effects of assuming pressures resulting from 100% release of fission gas and those obtained by using the experimental data.

For a 1-mil hole, approximately 60 sec are required to expel all the sodium bond at a burnup of 10,000 MWd/MT (assuming a gas pressure equivalent to 100% release of fission gas). At 50,000 MWd/MT, this time is reduced to approximately 47 sec. The use of experimental data increases the time for bond release by approximately 25% (at a burnup of 50,000 MWd/MT).

Also noted in Fig. 16 are results for a hole size of 20 mils. In this case, the time to release the sodium bond at 50,000 MWd/MT would be reduced to 0.04 sec. For small hole sizes, a relatively long time (compared to time to cause fuel melting) is required to release the sodium-bond inventory, and for large hole sizes, the time is very short (compared to time for fuel melting). This effect is important when considering fission-gas release and the conditions for fault propagation.

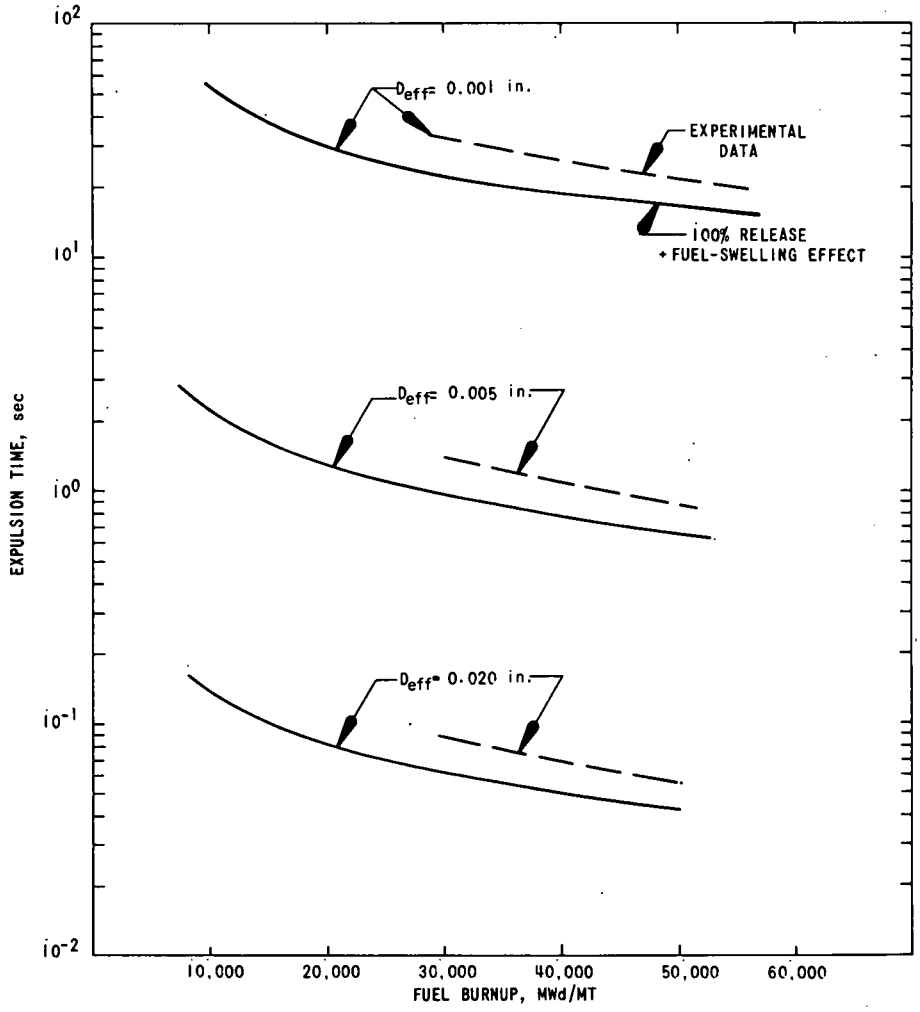

Fig. 16. Time to Expel Sodium Bond from a Mark-II Fuel Element, as a Function of Burnup and Size of Rupture Hole

Since the hole has been treated as an orifice, the discharge coefficient is an important variable. In Fig. 16, it was assumed that the discharge coefficient was equal to 1. Figure 17 shows the effect of reducing the discharge coefficient to 0.5. Reducing the discharge coefficient increases the expulsion times proportionately.

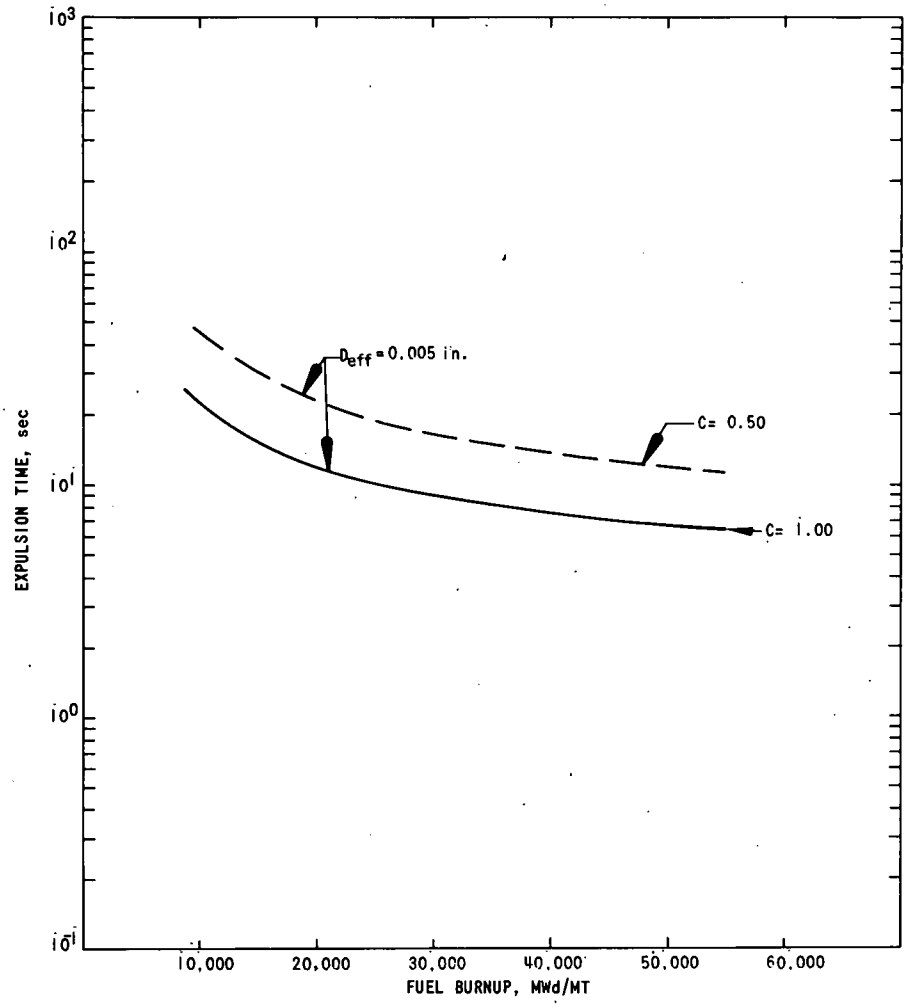

Fig. 17. Effect of Discharge Coefficient (C) on Time to Expel Sodium Bond from a Mark-II Fuel Element

In reviewing sodium-bond release, note that EBR-II has a fission-gas monitor (FGM) capable of detecting the release of fission-product gases to the system. The FGM can detect releases of fission gases following leakage of sodium bond, and will give an audible alarm in the reactor control room when this occurs. The FGM response may be delayed as long as 10 min, however, because of the time required for transport of fission products to the reactor cover gas and from there to the detectors of the FGM. (Another EBR-II instrument, the fuel-element rupture detector (FERD), detects delayed-neutron activity in a side stream of primary sodium. The FERD has a faster response than the FGM, but is not considered in this example.) Figure 18 shows, as a function of burnup and fission-gas pressure, the maximum diameter of the rupture hole for which the FGM would detect fission gas before all sodium bond has been expelled from a faulted fuel element (i.e., the diameter for which the expulsion time is 10 min). As Fig. 18 shows, for 100% release of fission gas at 10,000 MWd/MT, the hole diameter is 0.30 mil. At 50,000 MWd/MT, the hole diameter is reduced to less than 0.2 mil.

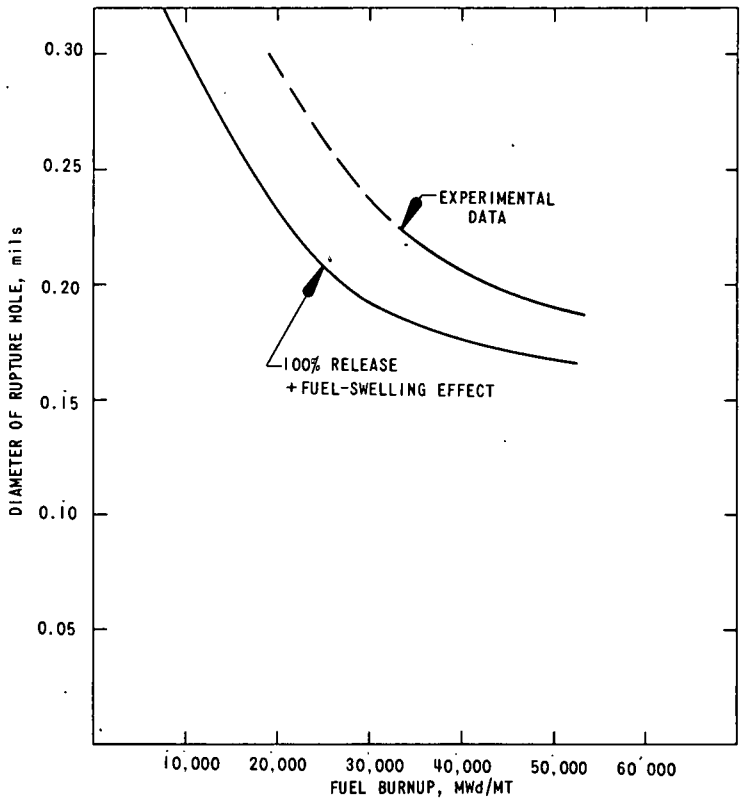

Fig. 18. Maximum Rupture-hole Diameter Permitting FGM Detection of Fission Gases from a Sodium-bond Leak, as a Function of Fuel Burnup and Fission-gas Pressure

In summary, for an effective hole diameter of 1 mil, 60 sec would be required to release all the sodium-bond inventory in a Mark-II fuel element with a burnup of 10,000 MWd/MT; this time would be reduced to less than 0.04 sec at 50,000 MWd/MT burnup. At the higher burnup, the effect of using experimental data for fission-gas release increases the time to expel all the sodium bond by a factor of 25%. Reducing the discharge coefficient from 1.0 to 0.5 doubles the time required for sodium expulsion.

D. Results of Studies of Fission-gas Dynamics

The theoretical model[4] for fission-gas release is similar to the model for sodium-bond release, except for the values used to simulate flow through a nozzle. A prime variable in the rate at which gas will flow through a cladding perforation (simulated by a nozzle) is the difference between the internal pressure in the fuel element and the external pressure of the reactor system. The internal fission-gas pressure was computed for the Mark-II fuel element by using two different assumed fission-gas-release percentages: (1) the experimental data depicted in Fig. 12, and (2) a 100% release of fission gas to the plenum, including allowance for the effect of fuel swelling in decreasing the volume of the gas plenum. (All pressure increases given in this report are assumed to occur at operating temperatures so that the zero point indicates the beginning of irradiation life.)

Figure 19 shows that the internal fission-gas pressure would be 200 psi at 10,000 MWd/MT and would increase to approximately 1600 psi at 50,000 MWd/MT, if all the gas produced were released to the plenum. On the experimental-data curve, very little fission-gas pressure is developed up to 20,000 MWd/MT, at which point the gas is released as the fuel matrix continues to swell outward to the cladding. At 30,000 MWd/MT, using the experimental data, the internal pressure would be 440 psi, increasing to approximately 950 psi at 50,000 MWd/MT.

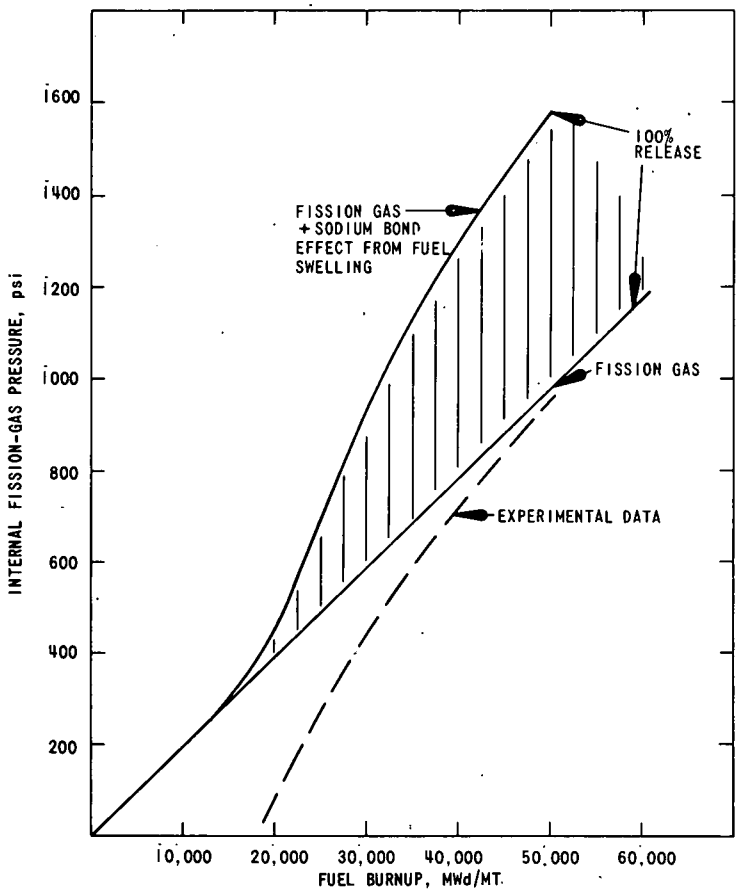

Fig. 19. Fission-gas Pressure in a Mark-II Fuel Element, as a Function of Gas-release Fraction and Fuel Burnup

An important variable to consider in the release of fission gas through a nozzle is the critical pressure ratio, the point at which sonic flow would develop through the nozzle or the perforation in the fuel cladding. In these studies, the fission gas was assumed to be mainly xenon and to behave like a perfect gas. The ratio (C_p/C_v) of specific heats of this gas was assumed to be 1.67, leading to a critical pressure ratio of 2.05. (See Appendix B for the method of calculation.) Figure 20 shows the pressure ratio as a function of fission-gas release fraction and fuel burnup for the Mark-II fuel element. For 100% gas release, the ratio is above the critical ratio at about 7500 MWd/MT and increases to approximately 30 at

50,000 MWd/MT. For the experimental data, the point of critical pressure ratio is not crossed until approximately 21,000 MWd/MT and increases to a value of 20 at 50,000 MWd/MT.

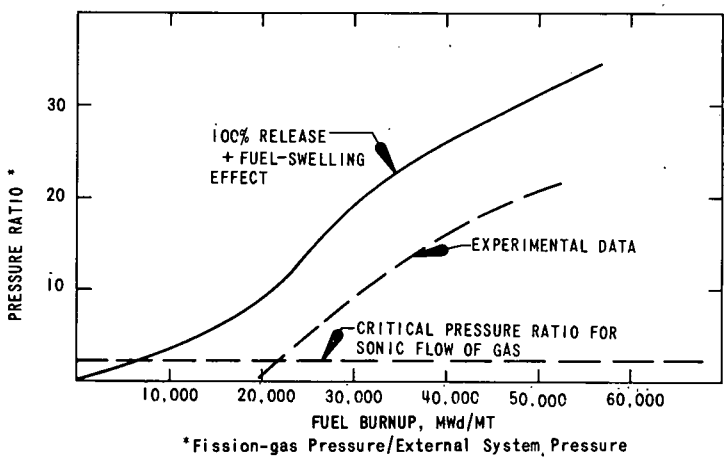

Fig. 20. Pressure Ratio as a Function of Fission-gas-release Fraction and Fuel Burnup

Using these pressure ratios, we calculated the percentage of subsonic flow at various burnups. (The results are plotted in Fig. 21.) For low burnups and 100% release of fission gas, approximately half the flow will be sonic and half subsonic. This proportion is reduced at 50,000 MWd/MT to only 10% of the flow being subsonic and 90% of the flow being sonic through the hole. Similar results are obtained by using

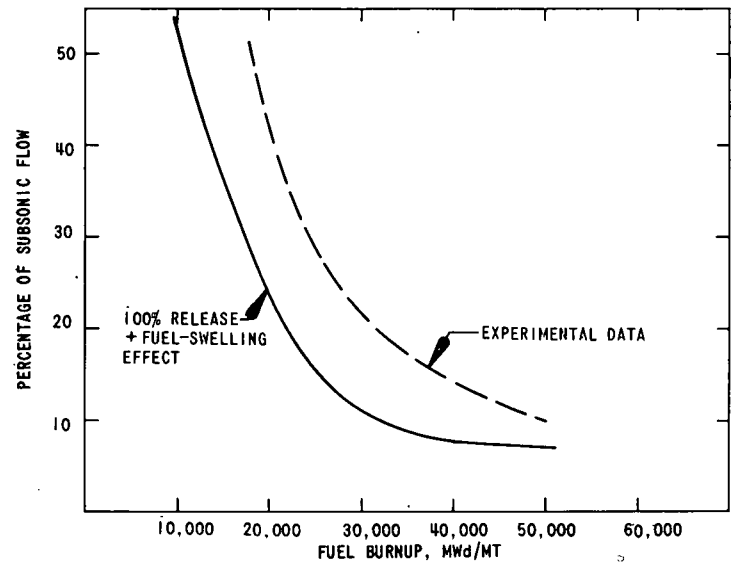

Fig. 21. Percentage of Subsonic Flow, as a Function of Fuel Burnup

the experimental fission-gas-release data. In the following calculations, only sonic flow of gas through the hole has been assumed to be capable of blocking the interstitial region around fuel elements. Therefore, only the sonic-velocity portion of the gas flow through the rupture hole is considered.

As indicated in Section III.C above, the hole size is extremely important in determining the conditions conducive to fault propagation by blanketing of adjacent pins with fission gas. Figure 22 shows the duration of gas flow at sonic velocities as a function of hole diameter, fuel burnup, and fission-gas-release fraction. The figure also shows the range of interest for fault propagation. This range was obtained by the following

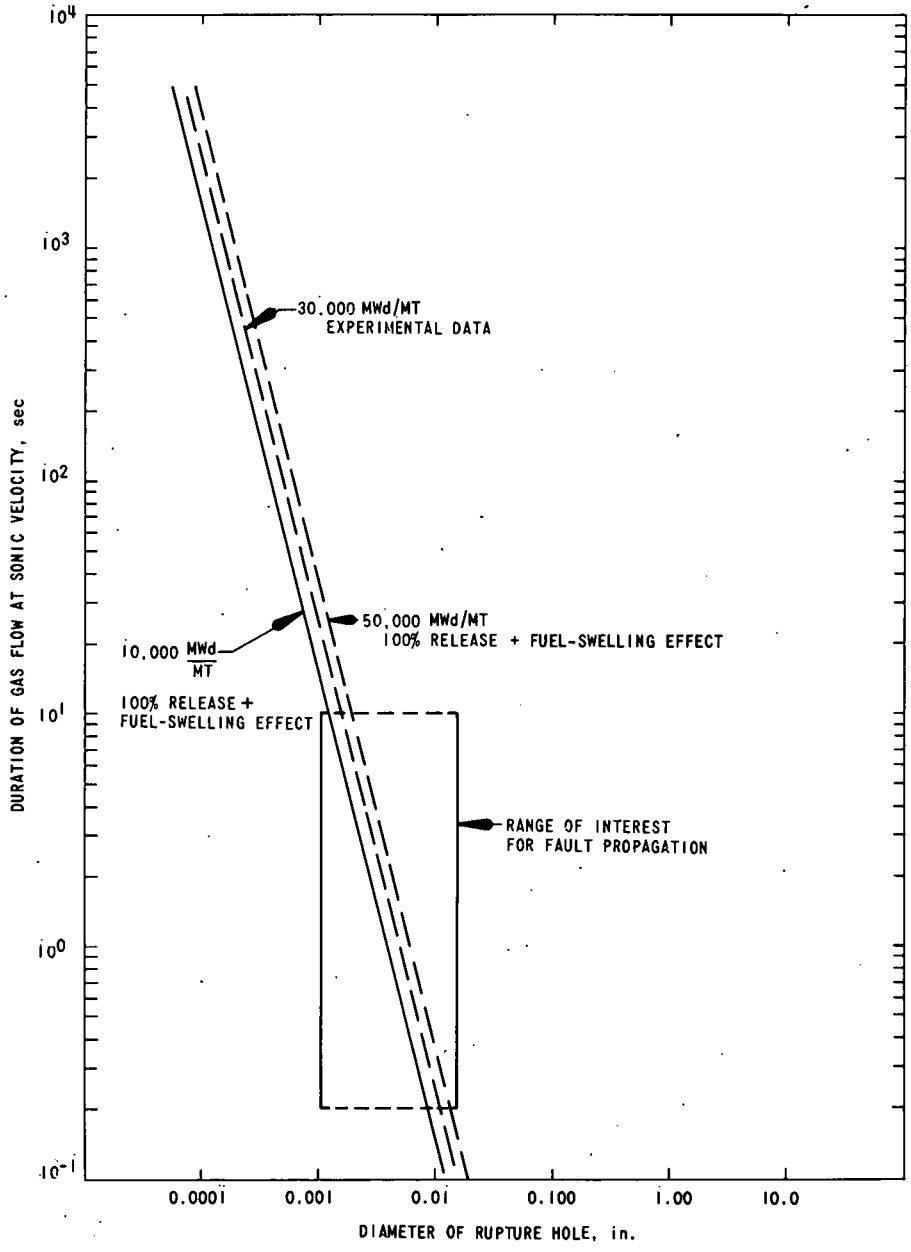

Fig. 22. Duration of Sonic Flow of Gas, as a Function of Hole Diameter, Fuel Burnup, and Fission-gas-release Fraction

process: Assuming complete isolation of a faulted Mark-II fuel element, we estimated from the material heat capacities[6,7] that without a sodium bond the temperature of the fuel in the element would rise at approximately 1265°F per sec. Assuming that the elements adjacent to this faulted fuel element are sodium bonded, we computed the temperature of the fuel in them to rise at a rate of approximately 932°F per sec. The lengths of time that adjacent fuel elements must be gas-blanketed to reach the temperatures at which sodium boiling, cladding failure, or fuel melting would occur were then calculated by assuming the following temperature thresholds: sodium boiling at 1700°F, cladding failure at 2000°F, and fuel melting at 2000°F. Table II gives the results and includes the time-to-failure values based on the results of TREAT transient experiments which indicate that a fuel element will fail when cladding temperatures reach the range of 1778 to 1859°F. By considering the sonic flow of gas out of the orifice, the gas expansion to the average system pressure of 30 psi at 1000°F, and the flowrate of primary sodium in Rows 4 and 5, where the experiments would be placed, we generated Figs. 23 and 24. These figures indicate the critical fission-gas-blockage time for fault propagation in EBR-II Mark-II fuel elements.

Using the results in Table II, we can determine when fuel melting, cladding failure, and sodium boiling could occur (assuming no internal pressurization of the fuel element in the case of sodium boiling). In practice, these conditions could occur only when the fuel has been burned to many tens of thousands of MWd/MT and contains a large supply of fission gas. Therefore, it is concluded that no sodium-bond boiling could occur in practice, owing to internal pressurization of the fuel element by fission gases. However, to obtain a lower limit of the range of interest, we assumed sodium-bond boiling at atmospheric conditions. As noted in Table II, this boiling would take place in 0.65 sec. To allow for uncertainties in the model and data, 0.2 sec has been taken as the lower limit, or the shortest time in which gas blanketing could induce cladding failure in adjacent pins. The upper limit for cladding failure is approximately 1 sec. In addition, Fig. 24 shows that at 50,000 MWd/MT the interstitial regions around fuel elements can be blocked for approximately 5 sec if the elements are located in Row 5. Allowing for uncertainties, this limit has been moved up to 10 sec. Thus, the critical range of interest for fault propagation from all burnups and fission-gas-release fractions considered included hole sizes from 1 mil (~10.0 sec of gas blanketing) to approximately

TABLE II. Times to Reach Failure Temperatures Following Gas Blanketing

Failure Mode	Starting Temp, °F	Failure Temp, °F	Time to Reach Failure Temp, sec
Sodium-bond boiling	1095	1700	0.65
Fuel melting	1175	2000	1.00
TREAT results	-	1778-1859	0.77-0.86

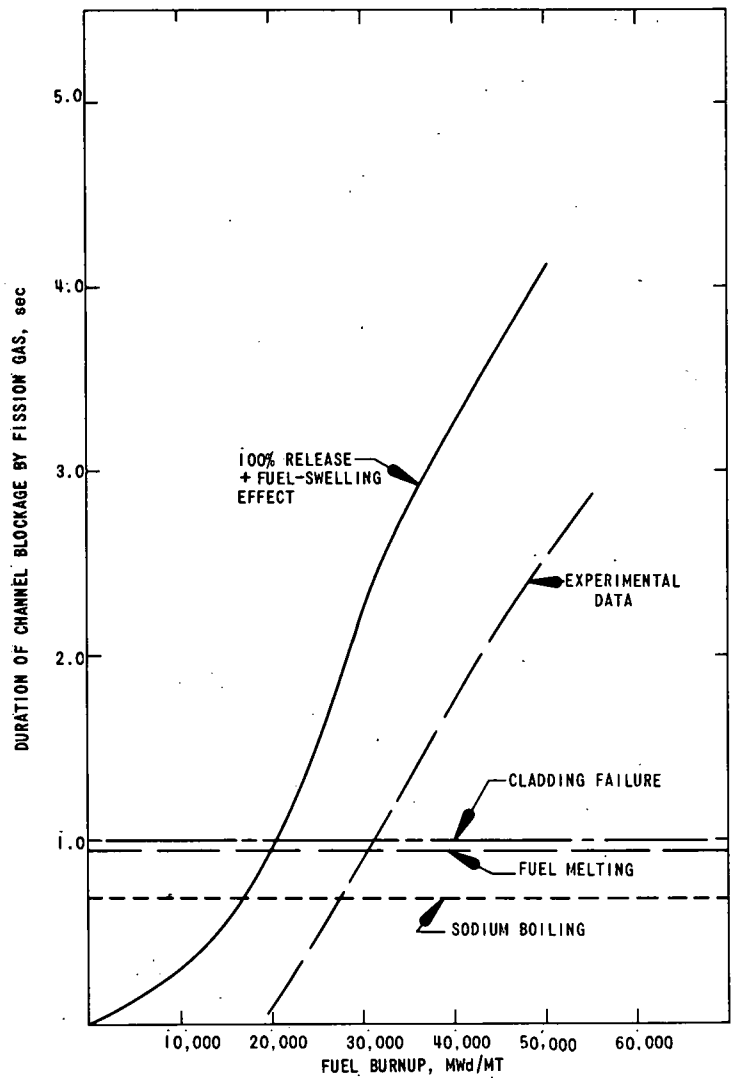

Fig. 23. Critical Fission-gas-blockage Durations for Fault Propagation in EBR-II Mark-II Subassemblies in Row 4

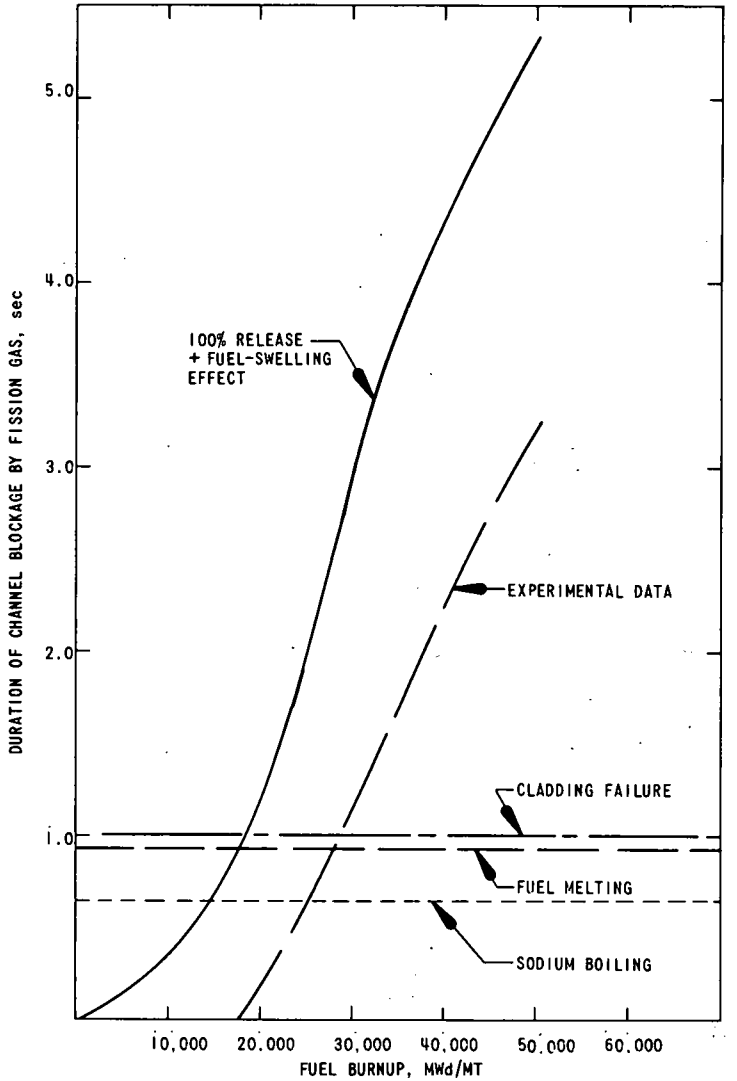

Fig. 24. Critical Fission-gas-blockage Durations for Fault Propagation in EBR-II Mark-II Subassemblies in Row 5

20 mils (~0.2 sec of gas blanketing) in effective diameter. As noted in Section III.C above, a perforation having an effective diameter of approximately 0.15 to 0.30 mil is sufficient for the fission-gas monitoring system to respond with an alarm before all sodium bond has been extruded from a faulted element. Thus the upper and lower time limits are physically bounded, so that the lower limit represents the shortest time in which material temperatures can rise enough to initiate a second failure in an adjacent element, and the upper limit is dictated by the volume of gas available at the highest burnup and by the response time of the detection system.

In summary, assuming 100% fission-gas release, the internal fission-gas pressure is approximately 400 psi at a burnup of 20,000 MWd/MT, and increases to 1600 psi at 50,000 MWd/MT. If the experimental data are used, these numbers are lower, yielding a maximum of approximately 950 psi at 50,000 MWd/MT. At burnups of 7500 MWd/MT or greater, the pressure ratio is higher than that required for sonic flow out of the nozzle, assuming xenon is a perfect gas. With the use of experimental data for fission-gas release, however, the pressure ratio does not exceed that required for sonic flow until burnup is well over 20,000 MWd/MT. For burnups greater than 30,000 MWd/MT, an appreciable amount of flow from the nozzle will be sonic. The time at sonic-flow velocities depends on hole size and pressure conditions. The critical range of interest for fault propagation has been identified as that which results from a rupture hole of 1 to 20 mils in effective diameter. If the fuel element is placed in Row 5, conditions of failure in adjacent fuel elements may be theoretically produced by blocking the coolant flow around these elements with gas for 0.65 to 1 sec. The conditions for fault propagation are discussed in some detail in Section IV.

E. Interaction of Sodium and Molten Fuel

The consequences of an interaction of sodium and molten fuel depend on the initial temperatures of liquid fuel and coolant, the properties of the fuel, and the volume of fuel and sodium involved. The model[5] described in the appendixes is definitely the worst upper-limit case. This model assumes that initially the fuel and sodium are mixed, at constant volume, and that temperature equilibrium is attained before expansion takes place. The mechanical-work potential is based on the assumption that thermal equilibrium exists at all times between the molten fuel and the mixture of sodium liquid and vapor. One of the critical parameters in this study is the maximum fuel temperature theoretically obtainable during a failure involving loss of bond. Assuming that (a) the initial operating temperature is approximately 1100°F in Row 5, (b) because of gas blanketing, the fuel temperature rises at a rate of 932°F/sec, and (c) gravity is the only force causing the fuel to flow downward and interact with the sodium bond, we can compute the worst temperature conditions at which interactions between sodium and molten fuel can occur. The time for the level of molten fuel to drop approximately 0.5 ft (worst case) under the force of gravity is approximately 0.2 sec. If we assume that the melting point of the fuel is 2000°F and that

the heat of fusion is equivalent to 509°F, the first point at which liquid fuel would be fully available for flow would be approximately 2500°F. Because it takes 0.2 sec for the fuel level to fall 0.5 ft and for the fuel to react with the sodium in the vicinity of the molten fuel, this temperature could increase to 2700°F if the fuel did not contact the cladding. This temperature, approximately 1700°K, is considered an upper limit for the fuel temperature in a partially bonded fuel element.

If a fuel element is essentially unbonded and swollen to the cladding and there is a failure, the melted fuel could eventually be forced out of the failure point. This model assumes that the fuel temperature could rise at approximately 1265°F/sec. If we assume 2000°F for the melting temperature and 509°F for the heat of fusion, and add 250°F (approximately) for additional heating before the fuel contacted the sodium, the maximum temperature achievable would be 2800°F (approximately 1800°K). In the studies reported here, the maximum range of interest for fuel temperatures is assumed to be between 1700 and 2000°K (allowing for uncertainties). These upper limits are the worst conceivable theoretical values.

Figure 25 shows the maximum work (W_{max}) from an interaction of sodium and molten fuel as a function of initial fuel temperature (taken as 1150°K). At a fuel temperature of 1700°K and a coolant temperature of

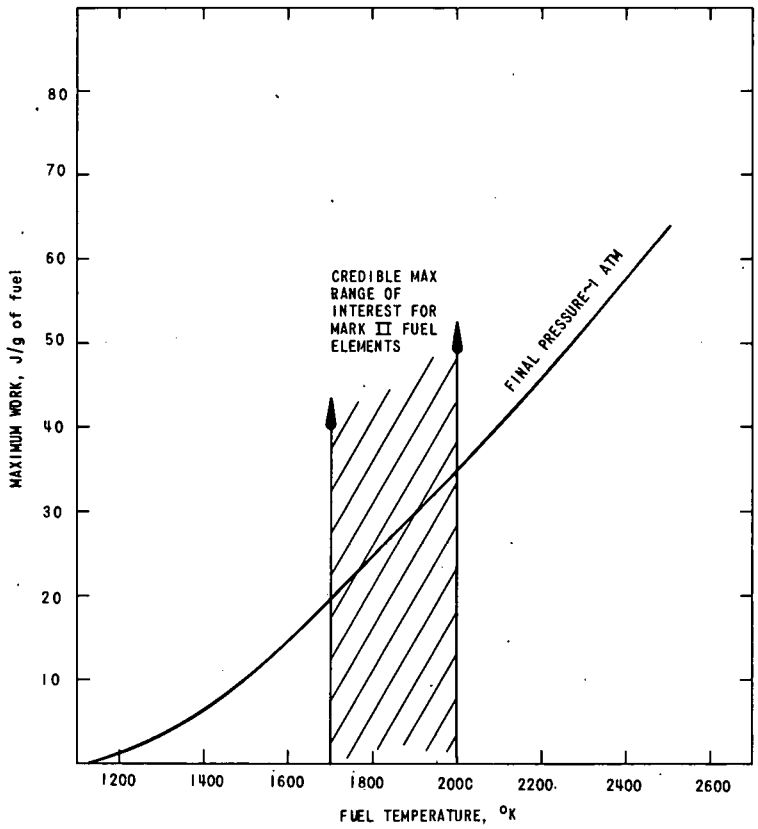

Fig. 25. Maximum Work from an Interaction of Sodium and Molten Fuel, as a Function of Initial Fuel Temperature (T_C = 1150°K)

1150°K, the maximum work would be 20 J/g of fuel. At 2000°K, this value rises to 35 J/g of fuel. The final pressure of the expanding vapor is 1 atm. Figure 26 shows the maximum work from an interaction of sodium and molten fuel as a function of the mass of sodium involved and the fuel temperature when the sodium temperature is held constant at 900°K. As the figure shows, the maximum work possible for the various fuel temperatures peaks between 0.020 and 0.026 g of sodium per gram of fuel.

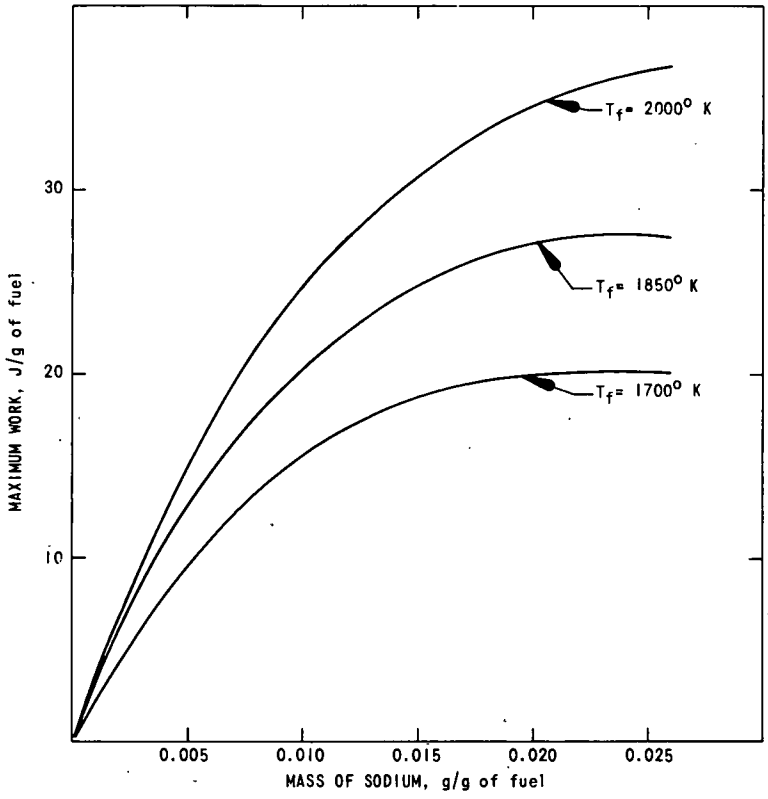

Fig. 26. Maximum Work from an Interaction of Sodium and Molten Fuel, as a Function of Mass of Sodium Involved and Fuel Temperature When Temperature Is Held Constant at 900°K

Figure 27 shows the effect of varying the coolant temperature. This figure gives the maximum work from an interaction of sodium and molten fuel as a function of initial temperatures of sodium and fuel. Increasing the initial fuel temperature from 1700 to 2000°K at a steady 900°K sodium temperature increases the work from 20 to approximately 35 J/g of fuel, or by a factor of less than two. At a constant fuel temperature of 1700°K, but with the coolant temperature increased from 800 to 1150°K, the maximum work increases from 20 J/g of fuel to approximately 24 J/g of fuel, or approximately 20%. Figure 28 shows the maximum vapor pressures attainable using this intimate-mixing model. The maximum pressure is a function of fuel temperature, coolant temperature, and the mass of sodium reacting in the mixture. For a fuel temperature of 2000°K,

a coolant temperature of 1150°K, and a coolant mass of 0.005 g/g of fuel, the maximum pressure attainable is 74 atm, or approximately 1100 psi.

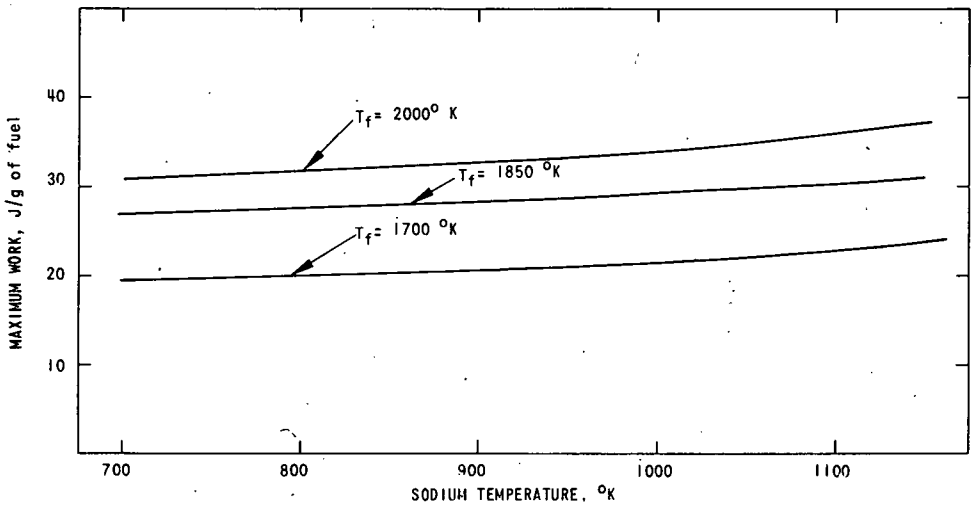

Fig. 27. Maximum Work from an Interaction of Sodium and Molten Fuel, as a Function of Initial Temperatures of Sodium and Fuel

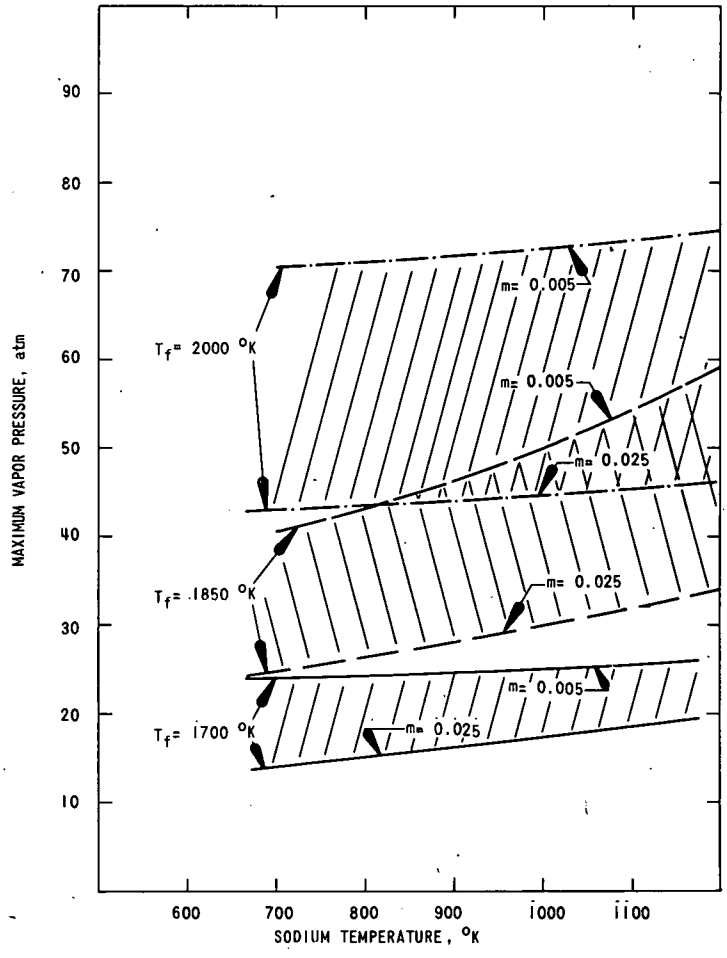

Fig. 28

Maximum Vapor Pressures from Interactions of Sodium and Molten Fuel, as a Function of Mass of Sodium (m) and Temperatures of Fuel and Sodium

TABLE III. Energy-conversion Efficiency (E) of Sodium/Molten Fuel Interaction at 900°K Coolant Temperature

Temp, °K	W_{max}, J/g of fuel	$E(W_{max}/E_f{}^a)$
1700	20.3	0.075
1850	27.3	0.093
2000	37.0	0.116

[a]Energy content in fuel at temperature shown.

Under these pessimistic conditions, it is interesting to note the energy-conversion efficiency of the sodium/molten fuel interaction. Table III presents the computed efficiencies based on the energy content of the fuel. At 1700°K, the efficiency is 7.5%; at 2000°K, the efficiency rises to approximately 12%. Therefore, under theoretical conditions, the efficiency of the interaction is no greater than 12% in the worst case considered. The effects of the interactions on surrounding fuel elements and on the hexagonal can of the subassembly are discussed in Section IV.

IV. CONDITIONS FOR FAULT PROPAGATION

A. Fission-gas Blanketing and Material Temperatures

Two basic modes of fault propagation are envisioned following a primary break in the cladding and a release of fission gas. These modes, depicted in Fig. 29, are:

1. A "burn-through" of the cladding of the adjacent element (caused by the impinging of a high-velocity jet of gas from the ruptured fuel element), followed by high temperatures from gas blanketing and leading to failure of cladding or fuel in additional adjacent fuel elements.

2. The release of fission gas from a failed fuel element and the subsequent gas blanketing of the axial interstitial regions between fuel elements and failure of adjacent fuel elements.

These two models have one thing in common: gas blanketing that results in higher-than-normal temperatures in fuel-element material. The THTB[8] generalized three-dimensional heat-transfer program was used to calculate the material temperatures resulting from partial gas blanketing of a Mark-II fuel element. In these calculations, two power levels (50 and 62.5 MWt) were used along with beginning- and end-of-life conditions of the Mark-II fuel pins. (In beginning-of-life conditions, a large sodium annulus is around the fuel pins; in end-of-life conditions, the fuel is swollen and is contacting the inner cladding surface, and the sodium bond is greatly reduced. Figures 30-33 show the detailed models and the maximum material temperatures resulting from these calculations. Figures 34-37 show the radial profiles obtained around the circumference of the fuel element. The worst conditions are achieved at end-of-life conditions and 62.5 MWt operation. As noted in Fig. 33, a sector greater than 200° must be gas-blanketed

before any part of the fuel pin will be in a melting condition. (With end-of-life conditions and high fast fluence on the cladding, cladding rupture may occur before fuel melting. However, fuel melting is a well-defined point and will be used in the discussion under Section IV.A.)

The above results indicate that a sector greater than 200° must be blanketed with gas before any adjacent pin could reach a failure point leading to breaching of its cladding and the release of its inventory of fission gas under pressure. Figure 29 shows a typical arrangement of fuel elements in a Mark-II subassembly. The shaded areas indicate possible areas of gas blanketing resulting from various fuel-element ruptures. As the figure indicates, the location of the wire wrap would limit the gas blanketing resulting from a single rupture to a 180° sector of a fuel element. Under end-of-life conditions and 62.5 MWt, a 180° blanketing would result in a fuel and cladding temperature approaching 1650°F. It is questionable whether the cladding surface would rupture because of some unknown failure phenomenon. Under the conditions assumed, failure would not occur, and no fuel melting would be experienced. The radial temperature profiles (Fig. 37) indicate that only a small portion of the fuel at this degree of gas blanketing is

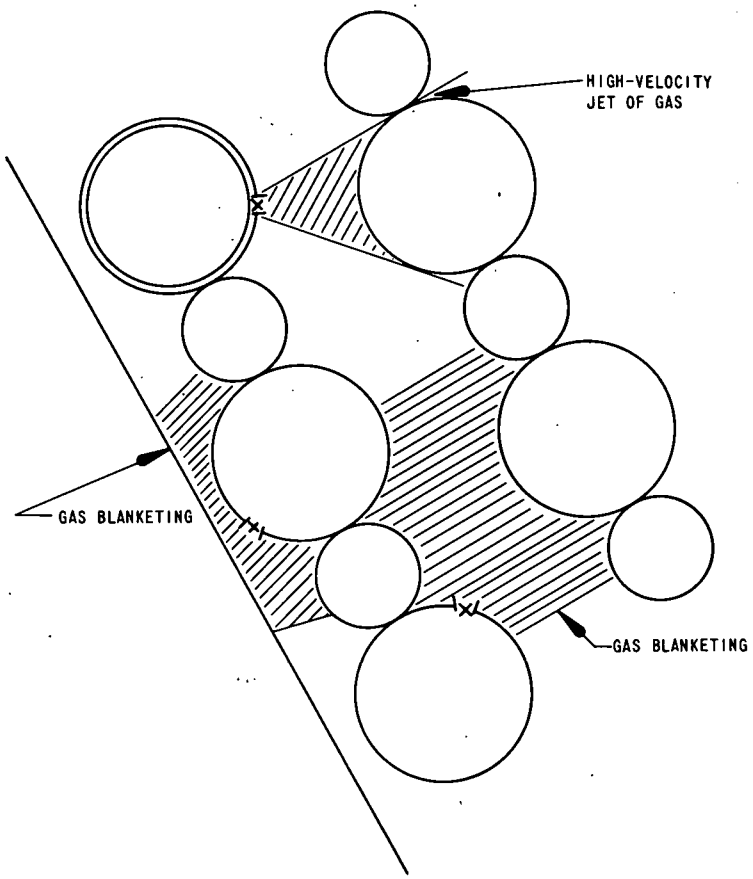

Fig. 29. Possible Modes of Fault Propagation Resulting from Fission-gas Blanketing in a Mark-II Subassembly

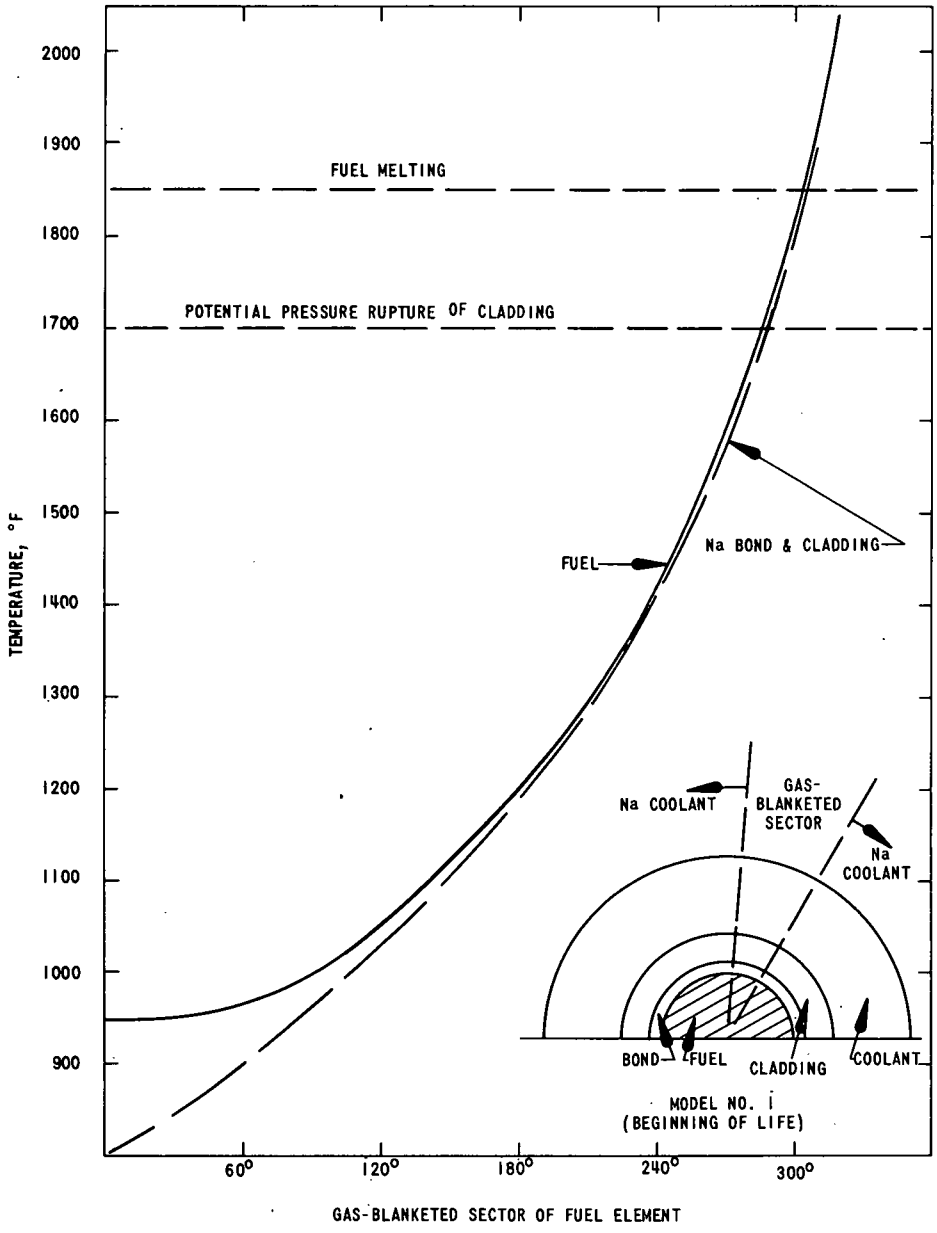

Fig. 30. Maximum Material Temperatures in a Mark-II Subassembly at 50 MWt, Following Fission-gas Blanketing of a Single Fuel Element at Beginning-of-life Conditions

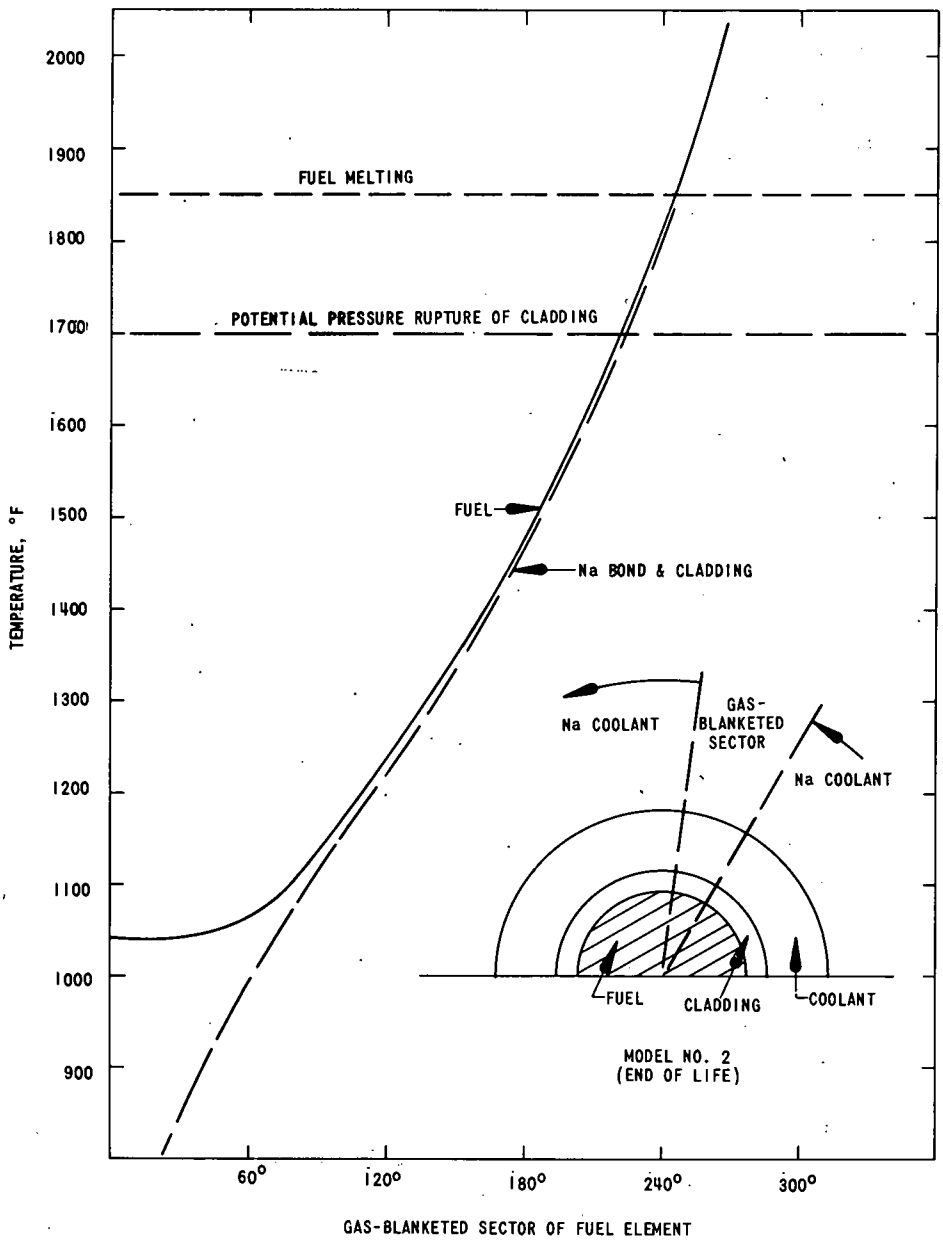

Fig. 31. Maximum Material Temperatures in a Mark-II Subassembly at 50 MWt, Following Fission-gas Blanketing of a Single Fuel Element at End-of-life Conditions

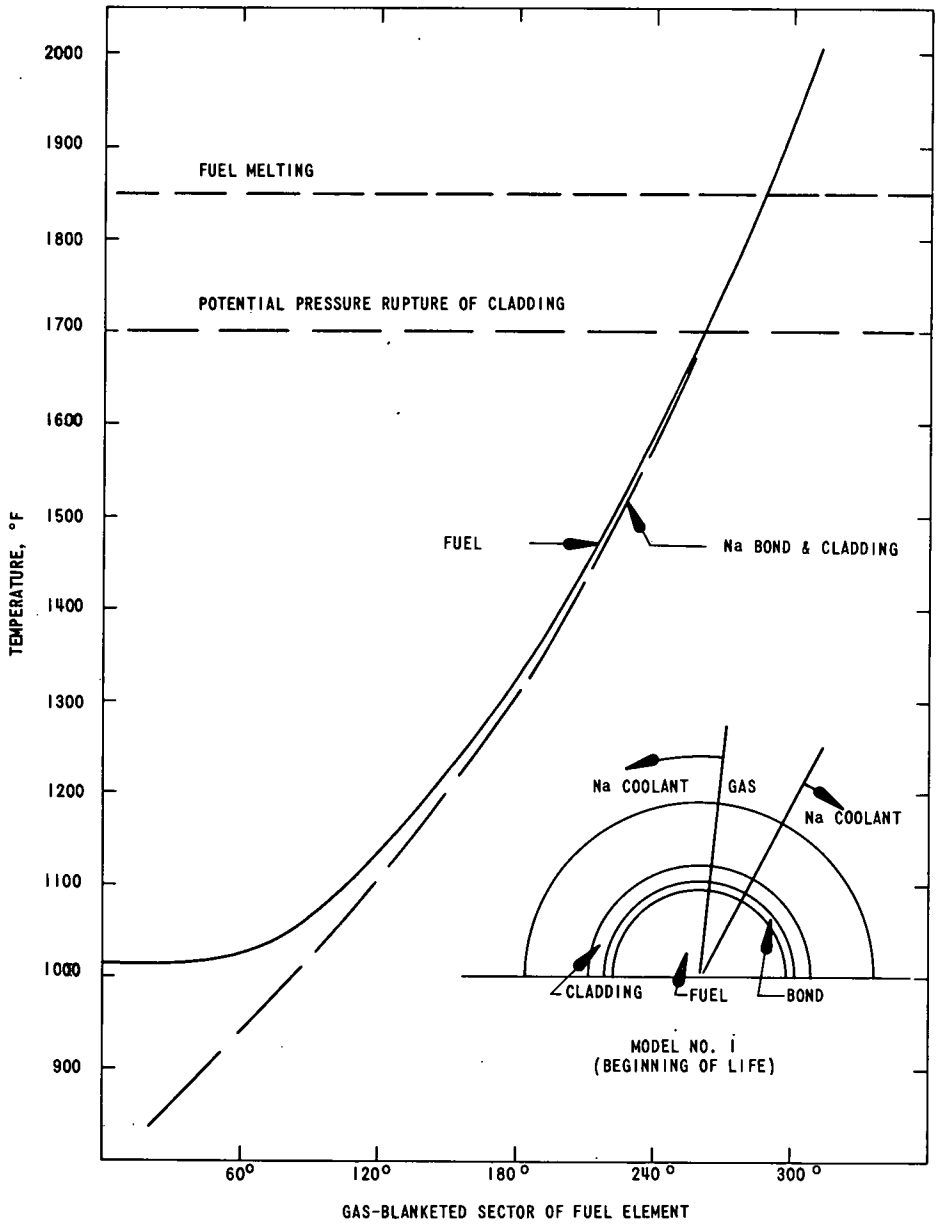

Fig. 32. Maximum Material Temperatures in a Mark-II Subassembly at 62.5 MWt, Following Fission-gas Blanketing of a Single Fuel Element at Beginning-of-life Conditions

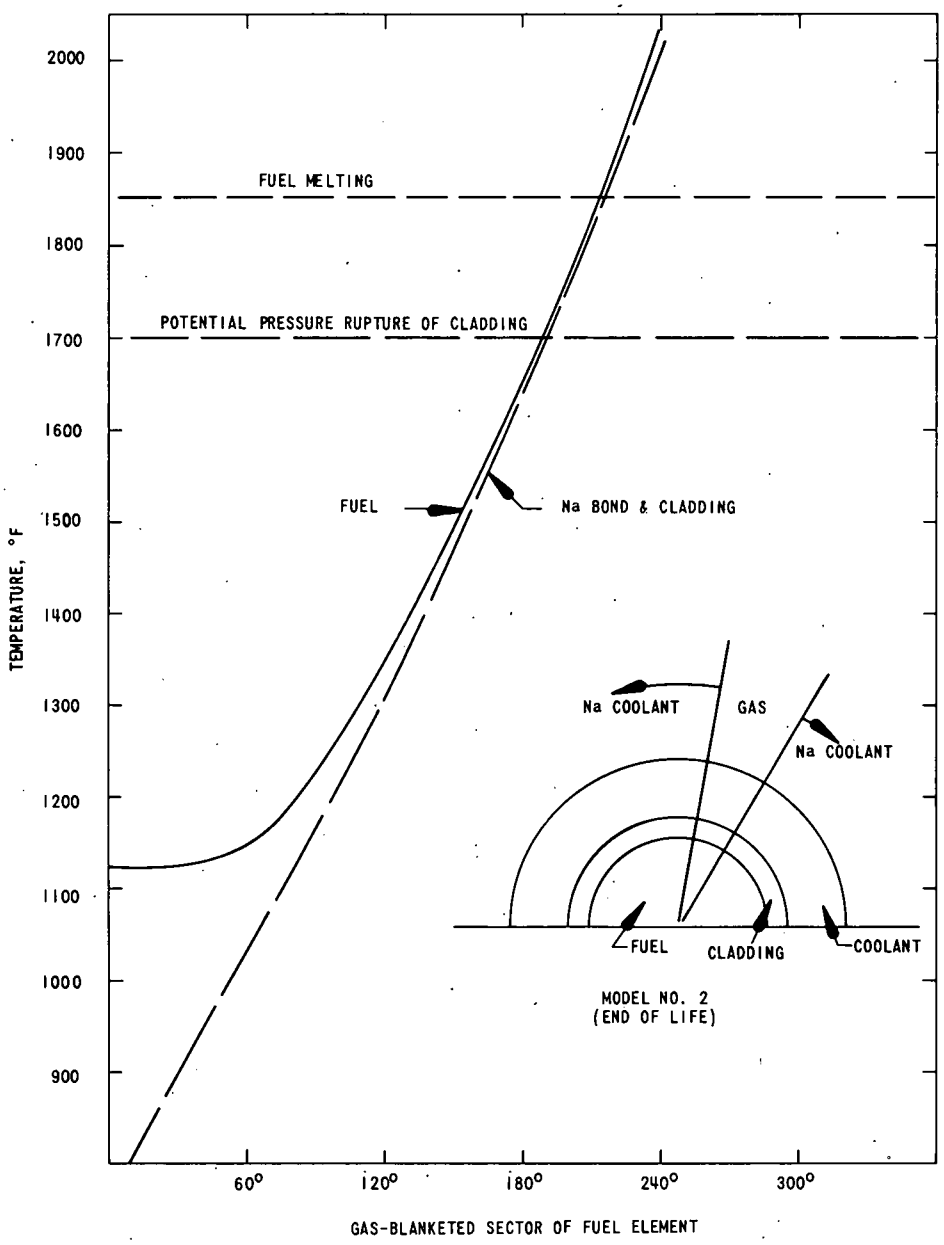

Fig. 33. Maximum Material Temperatures in a Mark-II Subassembly at 62.5 MWt, Following Fission-gas Blanketing of a Single Fuel Element at End-of-life Conditions

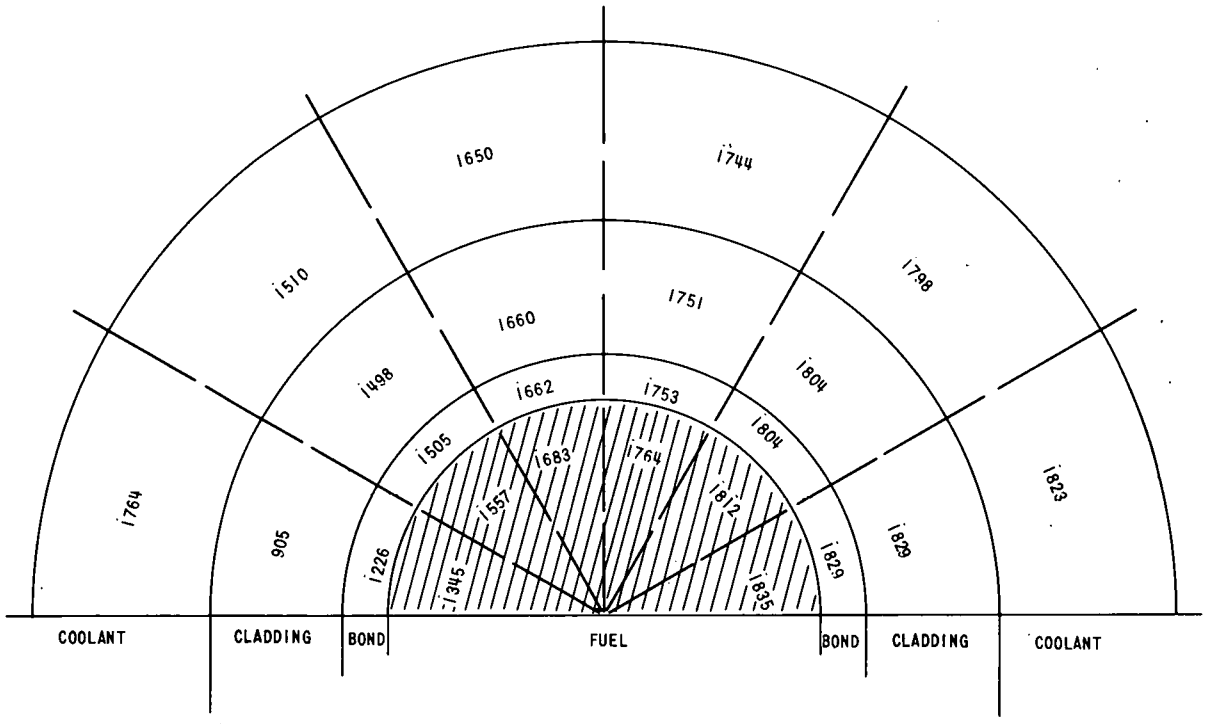

Fig. 34. Radial Temperature Profile in a Mark-II Fuel Element: 300° Gas Blanketing, 50 MWt, Beginning-of-life Conditions (temperatures in °F)

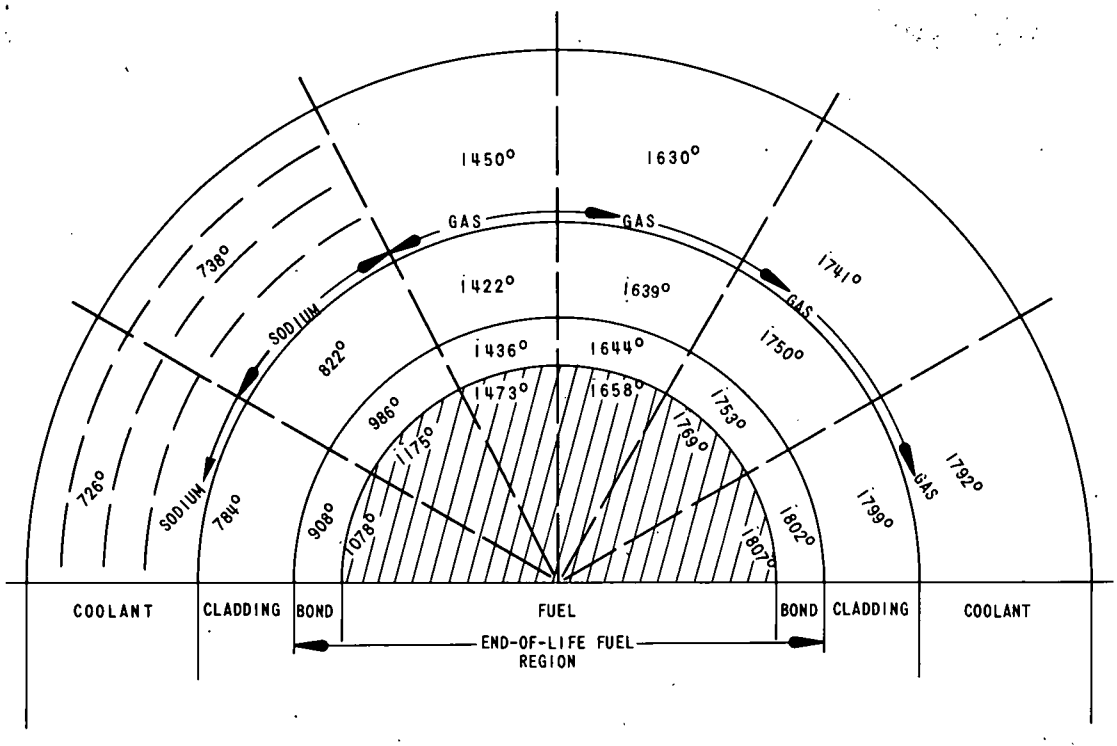

Fig. 35. Radial Temperature Profile in a Mark-II Fuel Element: 240° Gas Blanketing, 50 MWt, End-of-life Conditions (temperatures in °F)

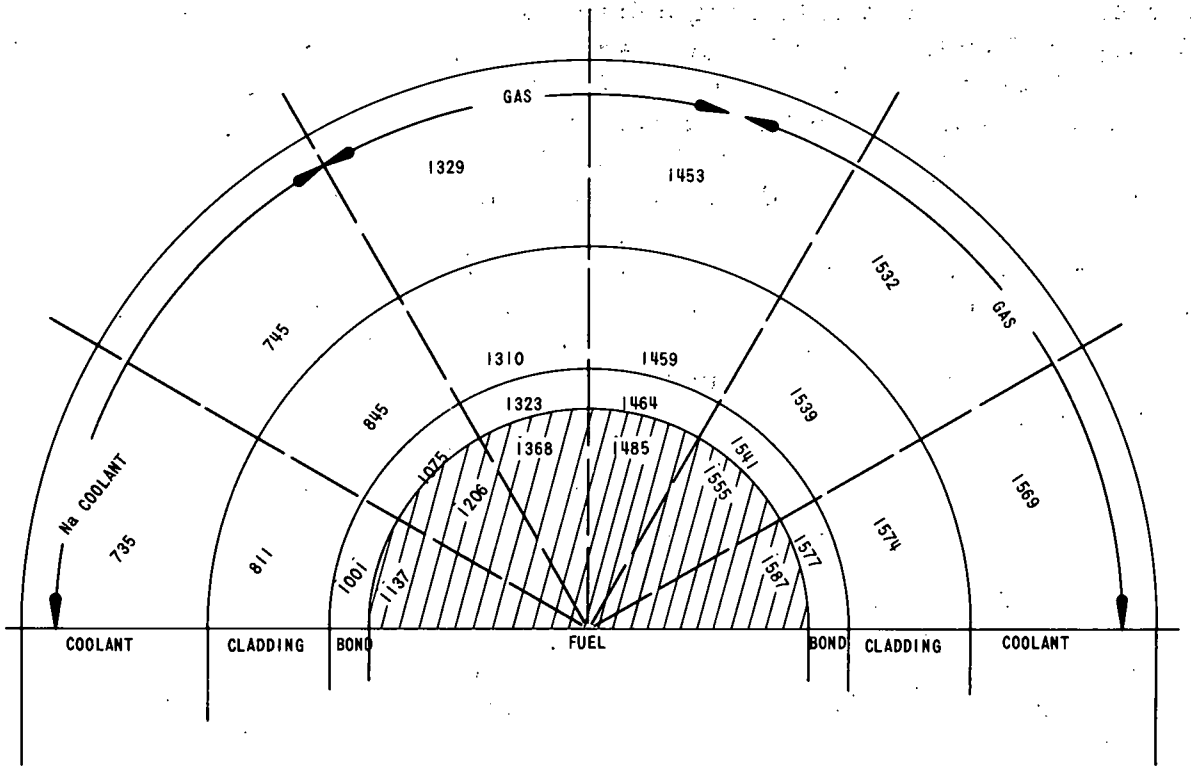

Fig. 36. Radial Temperature Profile in a Mark-II Fuel Element: 240° Gas Blanketing, 62.5 MWt, Beginning-of-life Conditions (temperatures in °F)

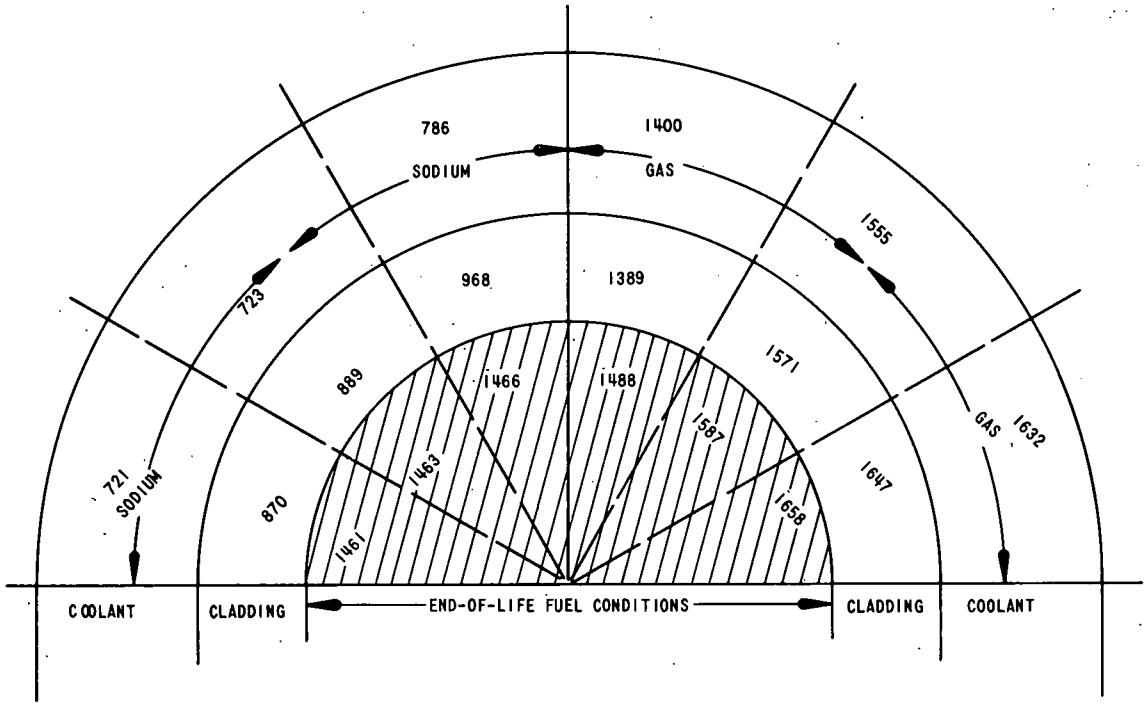

Fig. 37. Radial Temperature Profile in a Mark-II Fuel Element: 180° Gas Blanketing, 62.5 MWt, End-of-life Conditions (temperatures in °F)

approaching the normal melting point of U-5 w/o Fs. Using the classic Clapeyron Equation[9] relating the variation in melting point with pressure, we calculated the $\Delta T/\Delta P$ for U-5 w/o Fs to be about 0.05°C/atm. This is based on the assumption that the density of the liquid fuel is reduced by 5% of the density of the solid fuel. If a maximum internal pressure of approximately 100 atm is assumed, this would reduce the normal melting point by 5°C or 9°F (a small effect). However, this same internal fission-gas pressure greatly increases the effective boiling point of the sodium bond. The effective boiling point[10] of the sodium bond at 100 atm is calculated to be about 3100°F. Therefore, during those gas-blanketing transients that produce fuel melting, the sodium bond will not boil because of the high internal fission-gas pressures. This is not true at beginning-of-life conditions. In fact, the first point of failure would probably be the boiling of the bond in the early stages of irradiation. However, this is based on the assumption that there is some source of gas blanketing other than fission gas; there would not be sufficient fission gas to blanket the pins under early beginning-of-life conditions.

The above model is believed to be extremely pessimistic in that it assumes that the high-velocity jet of gas could uniformly blanket a surface of 180° or could keep the interstitial regions blanketed between several fuel elements. Owing to the highly turbulent flow within the Mark-II fuel subassembly, the gas being released could be dispelled, either because of the helical wire wrap or the turbulence inside the fuel subassembly. The preceding calculations indicate the extremely remote possibility of fault propagation due to gas blanketing of Mark-II fuel elements. The conditions under which gas blanketing could occur are extremely restricted even under worst-case conditions.

B. Interactions of Sodium and Molten Fuel, and Structural Analysis

This section deals with the interactions of sodium and molten fuel in the Mark-II fuel element following the initial rupture of the cladding and the slow release of sodium bond from the fuel element. A basic consideration in the calculations is the thermodynamic upper limits on conversion of thermal energy in the fuel to mechanical energy in the form of vaporization of the sodium bond. The results of some of the calculations of mixing U-5 w/o Fs and sodium in various mixtures were given in Section III, where it was pointed out that the maximum fuel temperatures achievable, as a credible upper limit, would range between 1700 and 2000°K. As noted in Fig. 25, this corresponds to a mechanical energy of 20-35 J/g of fuel involved.

The first part of this discussion will deal with these upper-limit values, considered to be the worst case. This initial discussion will be followed by a dynamic calculation of a loss of sodium bond and a detailed heat-transfer calculation resulting in material temperatures that would

be experienced during the initial loss of sodium bond in the Mark-II fuel element. These upper-limit calculations are based on the fact that thermal equilibrium exists instantaneously between the fuel and the liquid sodium and that this equilibrium remains throughout the expansion of the sodium vapor in the mixture.

The basic fault-propagation mode we are considering here involves a possible shock wave and subsequent gas pressure pushing on the interior of the Mark-II fuel subassembly. In assuming an instantaneous equilibrium, we have an energy release that is sufficiently high to transform liquid sodium into vapor at high temperatures and pressures. The subsequent high pressures can cause shock waves to propagate throughout the interior of the Mark-II subassembly. These shock waves and the subsequent expansion of the hot vapor behind the shock wave can cause damage to the adjacent fuel elements. The expansion of the shock wave is assumed to be spherical, and in such a case, the shock-wave energy in the vertical direction is normally taken to be two-thirds of the total, and in the radial direction, one-third of the total.

These assumptions then apply to the following structural analysis of the upper limit of damage:[11]

1. One-third of the total energy release is directed radially and must be accounted for by some kind of absorption mechanism. (It is also assumed that the escaping sodium vapor will do little damage, owing to condensation.)

2. To establish an extreme upper limit, the energy release is accompanied only by a shock wave.

Two energy-absorption mechanisms are considered:

1. Energy absorption by the stainless steel tubing and hexagonal can of the Mark-II subassembly.

2. Energy absorption by the stainless steel structure and the U-5 w/o Fs pins in the Mark-II fuel elements.

It is difficult to establish the geometric dissipation of energy in the subassembly, and the subsequent analysis will be based simply on the tensile strength of stainless steel in the Mark-II subassembly. The energy-absorption process envisioned in this structural analysis is simple strain of the material in absorbing the energy released from the interaction of sodium and molten fuel. (Details of this theoretical model are presented in Appendix D.) The basic model evaluates the equivalent weight of material required (as characterized by its tensile strength, allowable average elongation, and strain rate), and this equivalent weight is converted into the

number of fuel elements or subassemblies required to absorb the energy release from the assumed interaction of sodium and molten fuel. Figure 38 shows the assumed tensile strength of Type 304 stainless steel[12] as a function of temperature. In the subsequent analysis, three tensile strengths were assumed in order to cover a range of temperature and environmental uncertainties. These three tensile strengths are 50,000, 30,000, and 15,000 psi, which, according to Fig. 38, would cover temperatures of 1100 to 1600°F.

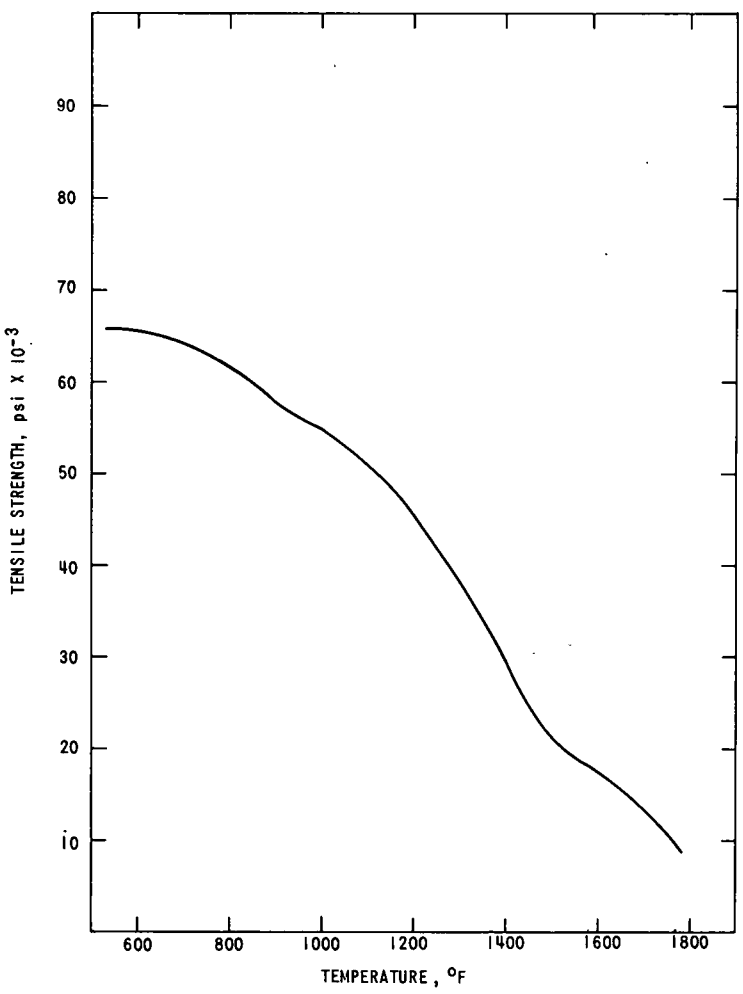

Fig. 38. Tensile Strength of Type 304 Stainless Steel, as a Function of Temperature

The equations listed in Appendix D were solved, and the results are graphically presented in Figs. 39-41 (these simple relationships are presented graphically for future reference). Figure 39 shows the simple conversion of energy release in inch-pounds to energy release in calories. Figure 40 presents the tensile strength of Type 304 stainless steel as a function of the specific plastic energy of stainless steel. Figure 41 indicates the variation of specific plastic energy of stainless steel as a function of the total strain of the material.

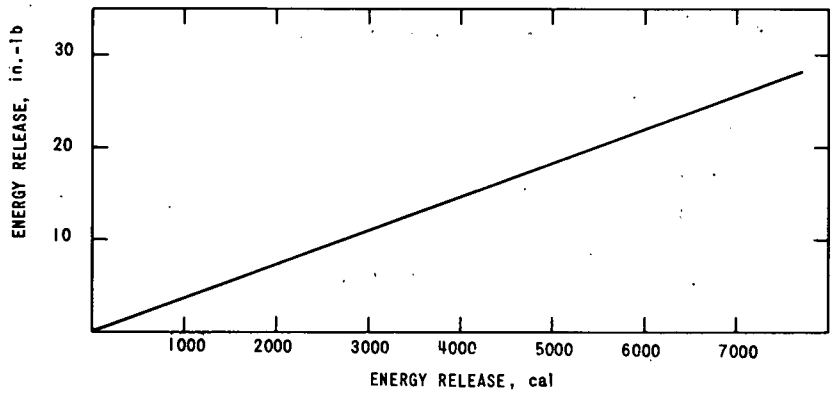

Fig. 39. Conversion of Total Radial Energy Release from Inch-Pounds to Calories

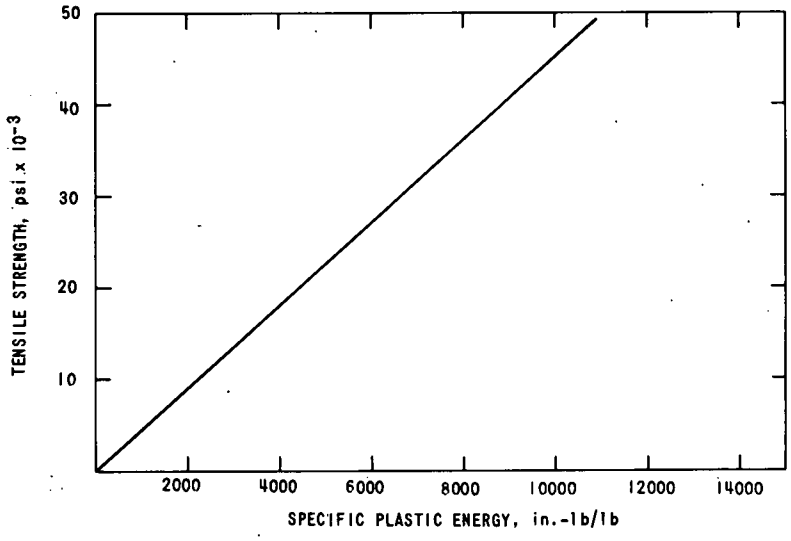

Fig. 40. Tensile Strength of Type 304 Stainless Steel, as a Function of Specific Plastic Energy

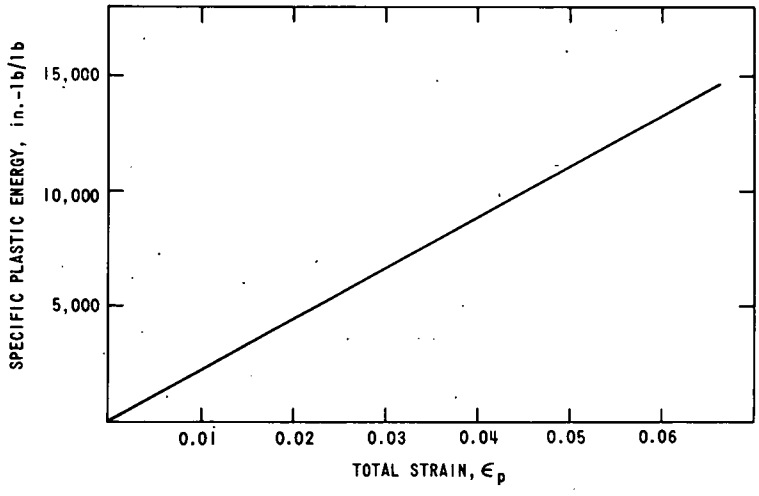

Fig. 41. Specific Plastic Energy of Type 304 Stainless Steel, as a Function of Total Strain

As indicated earlier, the maximum energy release expected from an interaction of sodium and molten fuel will range between 20 and 35 J/g of fuel involved. The upper limit of the amount of fuel involved is taken in these calculations to be the total inventory in one fuel pin. This is approximately 55 g of fuel, which converts to a total energy release of 4600 to 8000 cal. Using the relationships presented in Appendix D and various tensile strengths of the material involved in the absorption process, Fig. 42 presents the total weight of stainless steel required to absorb the energy release. If the tensile strength of stainless steel is 50,000 psi and the energy release is 4600 cal, approximately 5 lb of stainless steel are required to absorb this energy and dissipate it through strain in Type 304 stainless steel. If the tensile strength is reduced to 15,000 psi, the required mass of stainless steel is increased to approximately 17 lb.

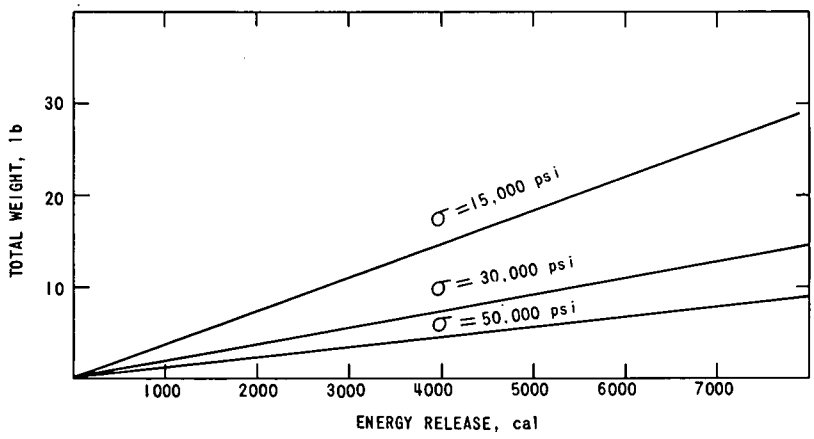

Fig. 42. Total Weight of Type 304 Stainless Steel Required to Absorb Energy Release, as a Function of Total Energy Release and Tensile Strength (σ)

In an average Mark-II subassembly, the average weight of stainless steel in the core region available for energy absorption is approximately 3.5 lb. Using this value, one can compute the number of subassemblies that may be affected by an energy release resulting from an interaction of sodium and molten fuel. Figure 43 shows the number of subassemblies affected vs the energy release when assuming only stainless steel as an absorbing medium. The figure includes the effect of tensile strength on the number of subassemblies affected. If the energy release is 4600 cal and the tensile strength is 50,000 psi, a maximum of 1.5 subassemblies will be affected by this interaction of sodium and molten fuel. If the tensile strength was reduced to 15,000 psi for the same 4600-cal energy release, the number of subassemblies affected would approach five.

If we now attempt to account for the effect of the fuel pins inside the tubing, we get the results depicted in Fig. 44. For the equivalent energy release of 4600 cal and an effective tensile strength of 50,000 psi, about three-fourths of a subassembly would be affected by this energy release.

These results are based on extremely conservative assumptions, on a simple structural-analysis model, and on upper limits based on rather severe assumptions. One reason for varying the tensile strength over the range chosen was the uncertainty of the fast fluence on the Mark-II cladding material as a function of time at temperature. These data are now being obtained and should be useful in future analyses.

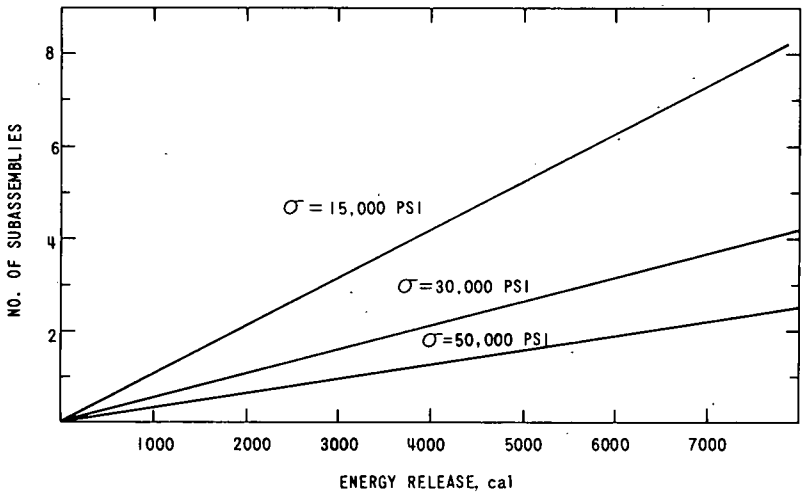

Fig. 43. Number of Affected Mark-II Subassemblies, as a Function of Energy Release and Tensile Strength (σ) When Only Stainless Steel Absorbs the Energy Released

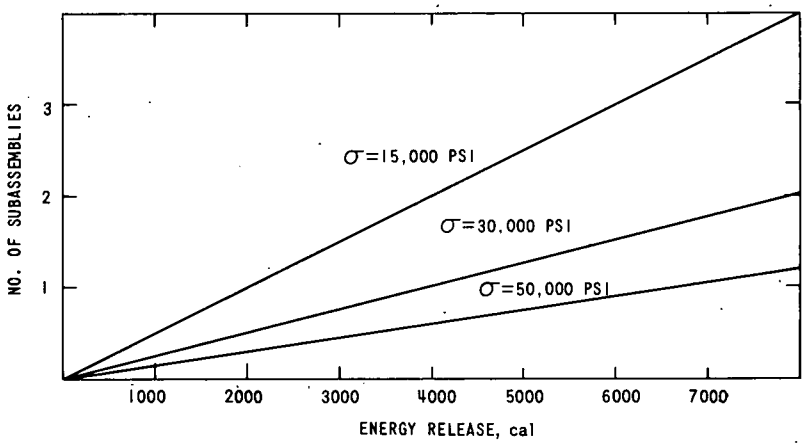

Fig. 44. Number of Affected Mark-II Subassemblies, as a Function of Energy Release and Tensile Strength (σ) When Stainless Steel and Fuel Absorb the Energy Released

Two key parameters in the above analysis are the fuel temperature and the volume of fuel involved in the interaction of the sodium and molten fuel. To place a more realistic limit on the expected interaction of sodium and molten fuel in a Mark-II element, the three-dimensional heat-transfer program (THTB) was used to compute the fuel temperature following the initiation of loss of sodium bond from the element. Figure 45 shows the

basic model considered in this analysis. As indicated, the only area subjected to a heat-transfer analysis was that portion of the tip of the fuel pin that was uncovered and partially bonded by fission gas to the cladding and flowing coolant while the remainder of the pin remained bonded by sodium to the cladding and flowing coolant. Two power levels (50 and 62.5 MWt) were considered in these analyses.

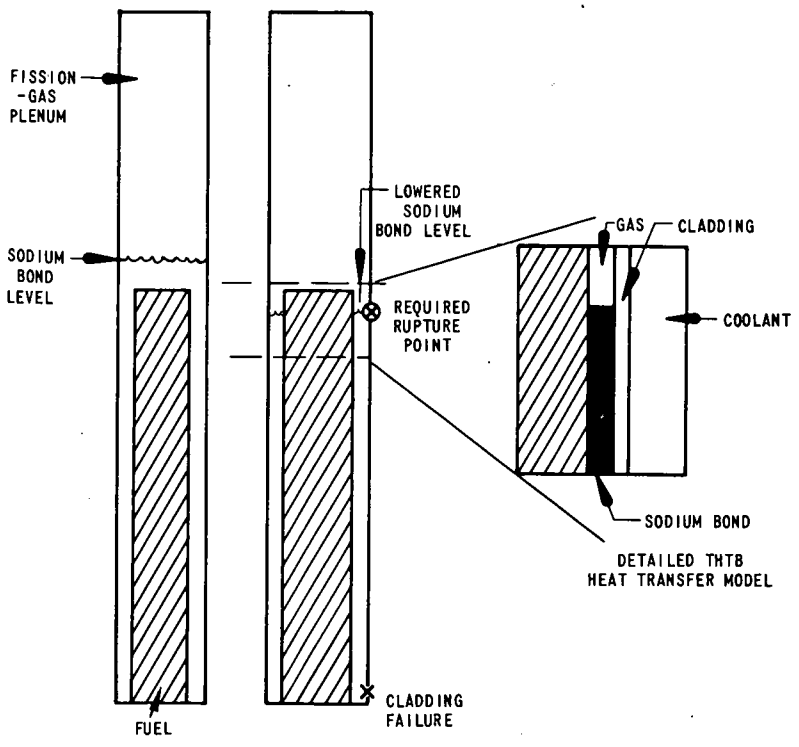

Fig. 45. Model for Sodium-bond Leakage and Conditions for Interaction of Sodium and Molten Fuel in a Mark-II Fuel Element (beginning-of-life conditions)

Parametric studies indicated that a very small portion of a pin would be at elevated temperatures following a loss of sodium bond. Figure 46 shows the results obtained from THTB heat-transfer calculations for 50-MWt operation and partial loss of sodium bond. In this analysis, the top 125 mils of the fuel pin was considered important. The resulting temperatures are indicated in the fuel, gas bond, cladding, and coolant regions. At 50-MWt steady-state operation, the maximum fuel temperature achievable was 1759°F. In the region bonded by fission gas, the maximum temperature achieved was 1362°F. The total height of the area considered was 625 mils, and the maximum sodium temperature in the bond region at 50 MWt was approximately 1070°F.

At 62.5 MWt, the conditions are different, as shown in Fig. 47. The maximum fuel temperature is 1950°F, and the gas-bond temperature exceeds 1460°F. The maximum sodium-bond temperature under these conditions is 1111°F. To compute the energy release resulting from the

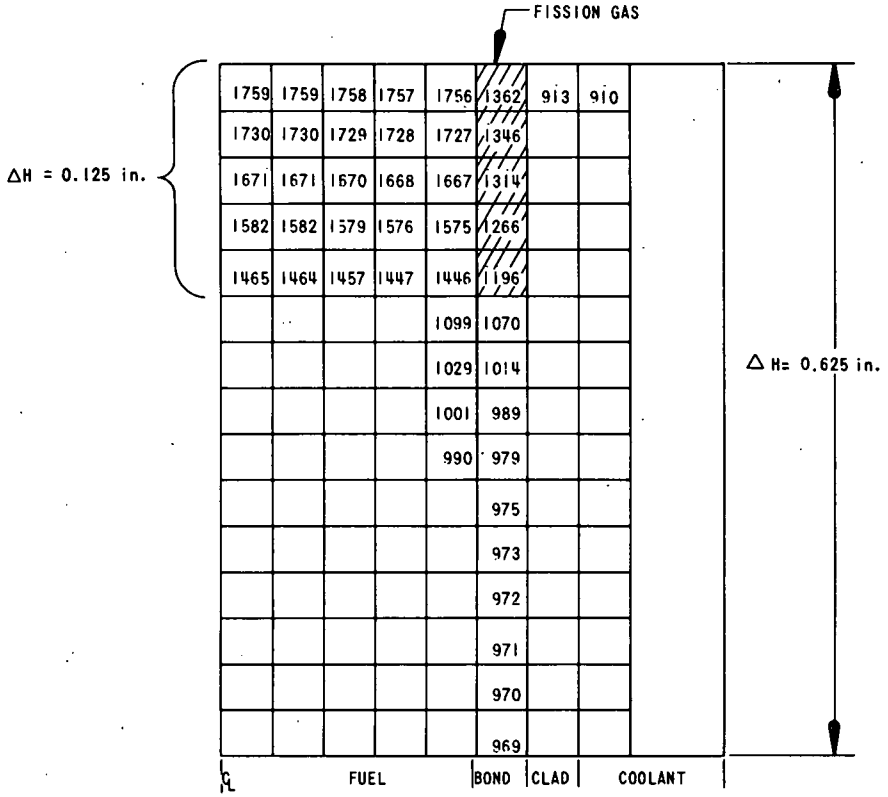

Fig. 46. Material Temperatures (°F) in a Mark-II Fuel Element Following a Drop in Sodium-bond Level and Gas Blanketing of Fuel Pin at 50 MWt

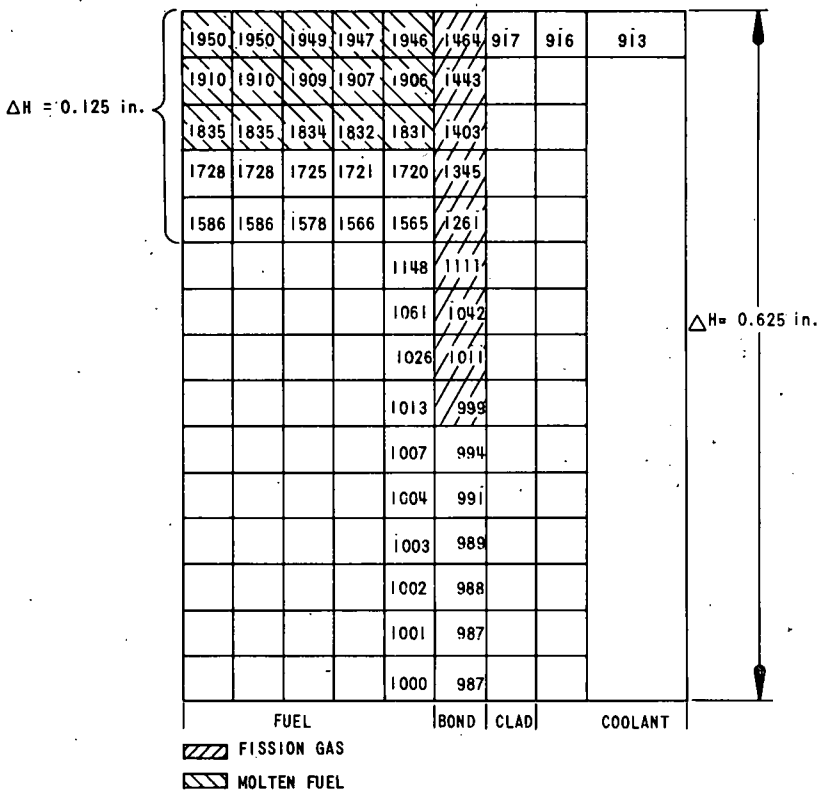

Fig. 47. Material Temperatures (°F) in a Mark-II Fuel Element Following a Drop in Sodium-bond Level and Gas Blanketing of Fuel Pin at 62.5 MWt

mixing of the hottest fuel with the hottest coolant under these conditions, we have taken 1950°F as equivalent to 1400°K and 1111°F as equivalent to 900°K. Figures 25 and 27 show that, under these conditions, approximately 5.6 J/g or approximately 23 cal of energy would be released with the mixing of the hottest fuel with the volume of the hottest sodium coolant. Using the equations in Appendix D, we note that the radial energy release, equivalent to 25 cal, is approximately 309 in.-lb of energy. If we assume a tensile strength of 50,000 psi, which corresponds to a temperature of approximately 1100°F, the equivalent mass of stainless steel required to absorb this energy release is about 0.028 lb. This required amount of steel would indicate that only one fuel element would be affected in a subassembly of 91 elements. Allowing for uncertainties due to the effects of fast fluence on the cladding material, one of the adjacent elements might also be involved because of this interaction of sodium and molten fuel.

The interaction of sodium and molten fuel requires sodium boiling and vapor formation and hence is dependent on fission-gas pressure. The reason for this is the effect of internal fission-gas pressure on the sodium boiling temperature. The above analysis assumed atmospheric pressure. Figure 48 shows the sodium vapor pressure as a function of temperature.

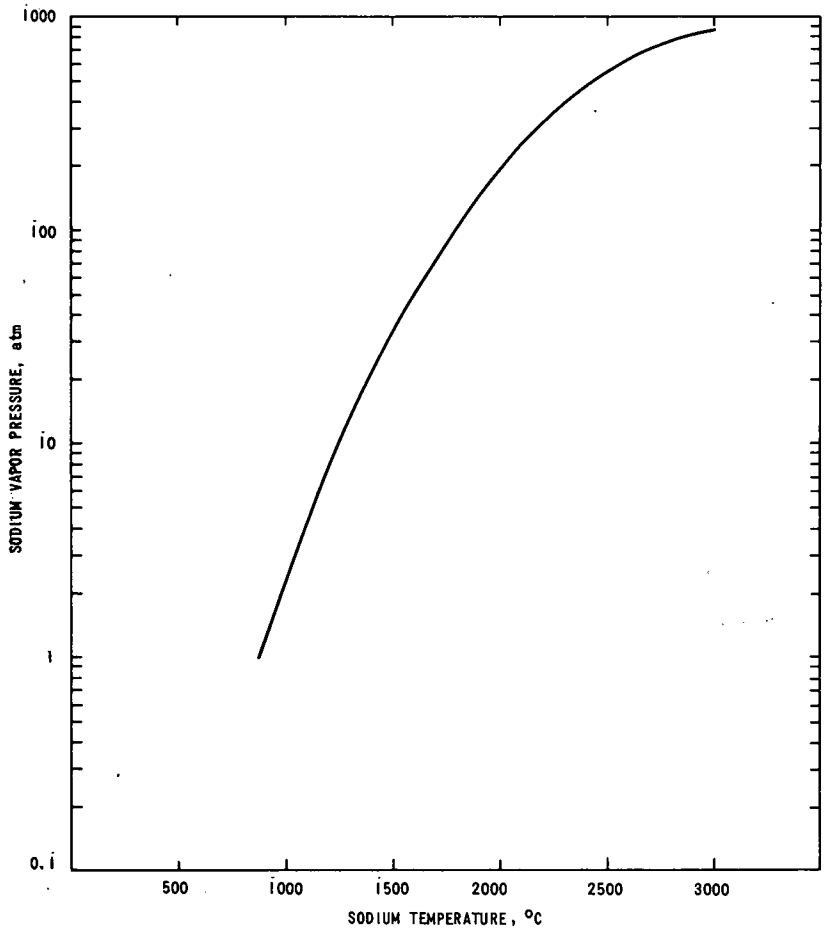

Fig. 48. Sodium Vapor Pressure as a Function of Temperature

As noted in Section III.D, a pressure of 1600 psi may be experienced near the end-of-life conditions. This is equivalent to approximately 100 atm, a pressure corresponding to a sodium boiling point of approximately 1800°C. Because the fuel would melt at approximately 1100°C in this postulated failure, no sodium vapor would be formed in the presence of a high fission-gas pressure. Therefore the calculations presented above assumed the atmospheric boiling point of sodium. This assumption implies physically that the rupture hole must be at the level of the interface of the sodium bond and the molten fuel and that fission-gas pressure must be absent so that sodium vapor would form.

If the break was located at the bottom of the fuel element, then we would have the possibility of superheating the sodium bond (assuming no heat loss to the flowing sodium), but would have little or no formation of sodium vapor within the fuel element if there was any fission-gas pressure. The maximum temperature being used for computation in the above analysis is 1100°C, corresponding to a sodium vapor pressure of approximately 4 atm. Assuming 100% release of fission gas, 4 atm of fission-gas pressure would correspond to a fuel burnup of about 2500 MWd/MT. If we use the experimentally measured fission-gas release and swelling rate for Mark-II type fuel, 4 atm of fission-gas pressure would correspond to a fuel burnup of approximately 20,000 MWd/MT. These results indicate that the fault-propagation mode involving interaction of sodium and molten fuel is most severe at the beginning-of-life conditions, when the fission-gas pressures are low, as opposed to the gas-blanketing mode, which is most severe at the end-of-life conditions, when the fission-gas pressures are extremely high.

V. CONCLUSIONS

This report considered two modes of fault propagation under steady-state operating conditions. There are (a) fission-gas blanketing of adjacent fuel elements resulting from an initial cladding failure, and (b) interaction of sodium and molten fuel within a fuel element, resulting from a loss of sodium bond. The conditions for fault propagation are well defined on the basis of the physical properties of the Mark-II fuel element and of the EBR-II reactor.

A. Fault Propagation by Fission-gas Blanketing Mode

For the fission-gas blanketing, the following conclusions can be listed:

1. Detection by the fission-gas monitor of fission gases following a sodium-bond leak before all sodium bond is lost from the element requires the diameter of the rupture hole to be less than 0.15 to 0.30 mil, assuming a circular hole. This would provide a 10-min transport delay time for the fission-gas monitor to respond.

2. Depending on the assumptions of fission-gas-release fractions from the fuel pin to the gas plenum, gas pressures will vary up to approximately 1600 psi at end-of-life conditions and 50,000 MWd/MT. For the initial design burnup level of 20,000 MWd/MT, the worst fission-gas pressure would not exceed 500 psi. If the experimentally measured rates of fission-gas release and fuel swelling were used, the internal fission-gas pressure at end-of-life conditions and 50,000 MWd/MT would not exceed 1000 psi.

3. Sonic flow of gas out of the rupture hole could be achieved at burnups greater than 7500 MWd/MT, assuming a 100% release of fission gas. With experimental data, sonic flow could be achieved at a burnup of approximately 22,000 MWd/MT. At end-of-life conditions and 50,000 MWd/MT, the pressure ratio between internal gas pressure and external system pressure would be approximately 30, assuming 100% gas release, and would be approximately 20 if experimental data were used.

4. The percentage of flow from the elements that is subsonic would be extremely low at end-of-life conditions, approaching 10% for burnups in excess of 30,000 MWd/MT, so that over 80% of the flow out of the rupture hole would be at sonic velocities. The credible range of interest for fault propagation corresponds to hole diameters of approximately 1 to 20 mils.

5. Assuming worst-case heating conditions following gas blanketing of a fuel element, fuel melting could be experienced at approximately 20,000 MWd/MT, assuming 100% gas release, and at 30,000 MWd/MT, assuming experimental data for fission-gas release.

6. At 62.5-MWt operating conditions, approximately a 200° arc of the surface of the cladding must be blanketed with gas before the fuel reaches the melting point.

7. The most credible gas-blanketing sector, owing to the geometrical arrangement of fuel elements and wire wrapping in the subassembly, is that with a 180° arc. Therefore, it is concluded that, although the release of fission gas from a ruptured element could elevate the temperatures of surrounding fuel elements, the degree of gas blanketing would not raise the temperature in those elements to the point where they would fail.

8. Finally, if a failure did occur in adjacent elements, the failure would probably be upstream from the initial failure and the rupture hole would probably not fall in the restricted range of 1 to 20 mils in diameter.

B. Fault Propagation by Interaction of Sodium and Molten Fuel

Conclusions drawn from the studies of fault propagation by interaction of sodium and molten fuel resulting from partial loss of sodium bond are as follows:

1. The upper-limit fuel temperature achievable during a partial loss of sodium bond lies between 1700 and 2000°K, assuming worst-case conditions of no heat loss from the fuel pin (i.e., no radial-axial heat transfer).

2. Assuming the above temperature limits, and the formation of vapor and its expansion to 1 atm, the available work would vary between 20 and 35 J/g of fuel involved.

3. The maximum work would be achieved with a sodium-to-fuel weight ratio of approximately 0.025, assuming a fuel temperature of approximately 2000°K. (The actual weight ratio of sodium to fuel in the fuel element is approximately 0.021.)

4. The effect of fuel temperature is such that increasing the fuel temperature from 1700 to 2000°K increases the available maximum work energy from 20 to 35 J/g, or a factor of less than two.

5. Increasing the sodium temperature from 700°K to approximately 950°K increases the maximum work by approximately 20%.

6. Under the worst set of conditions for the worst case, the maximum pressure computed did not exceed 80 atm.

7. The total energy release that must be absorbed in the structure is between 4600 and 8000 cal under the worst set of conditions (i.e., the entire inventory of fuel and sodium in one fuel element interacts). On the basis of the simple model presented in Appendix D and a tensile strength of 50,000 psi, the number of subassemblies affected by the interaction of the total inventory of fuel and sodium in one fuel element would be between 1.5 and 2.5. If the tensile strength were reduced to 15,000 psi, approximately five to eight subassemblies could be affected by the shock wave. These results are based on using only stainless steel as an absorbing medium. If credit were taken for the fuel inside the element, these numbers would be lower.

8. Based on a three-dimensional heat-transfer model, the maximum fuel temperature achieved at 62.5-MWt operation is 1950°F. The maximum sodium temperature at the interface of the fission gas and the sodium bond is 1111°F. These numbers correspond to a fuel temperature of 1400°K and a sodium temperature of 900°K. The volume of fuel involved in the postulated failure is computed to be 0.016 cc, equivalent to approximately 0.3 g. Allowing for uncertainties, the maximum amount of fuel available for interaction with sodium is assumed to be approximately 1 g.

9. At a fuel temperature of 1400°K and a coolant temperature of 900°K, the total work available would be 5.6 J/g (assuming that 1 g of fuel interacting at the optimum sodium-to-fuel ratio would yield an energy release of 5.6 J), or approximately 23 cal. Assuming 25 cal to include

uncertainties, a stainless steel mass of 0.028 lb would be required to absorb the energy release, at a tensile strength of 50,000 psi. This would correspond to less than one fuel element. Allowing for uncertainties in tensile strength, more than one fuel element could be involved in the effects of the interaction of sodium and molten fuel.

10. Because the structural analysis assumes that the energy is released instantaneously, the above limits are considered to be extreme upper limits. Most probably the energy release from an interaction of sodium and molten fuel would proceed much more slowly and the shock wave would be greatly reduced; therefore, it is concluded that only one fuel element would be involved in this loss-of-sodium-bond incident.

C. Proposed Experimental Programs

The results of this study have defined a fairly narrow range of conditions to be studied in assessing the effects of fission-gas blanketing or interaction of sodium and molten fuel in Mark-II fuel elements. It is proposed that model tests be constructed for operation in the TREAT experimental reactor to test the variables defined in this report and to assess the upper-limit values of material temperature, energy release, and structural damage. Very little damage would probably be experienced in these TREAT tests and subsequent EBR-II tests; confidence in the inherent safety of the Mark-II fuel-element design would thereby be increased.

APPENDIX A

Flow of Sodium Bond out of a Cladding Rupture

The flowrate of sodium bond was computed by assuming that the cladding rupture hole was a thin-plate orifice[4] (as shown in Fig. 49).

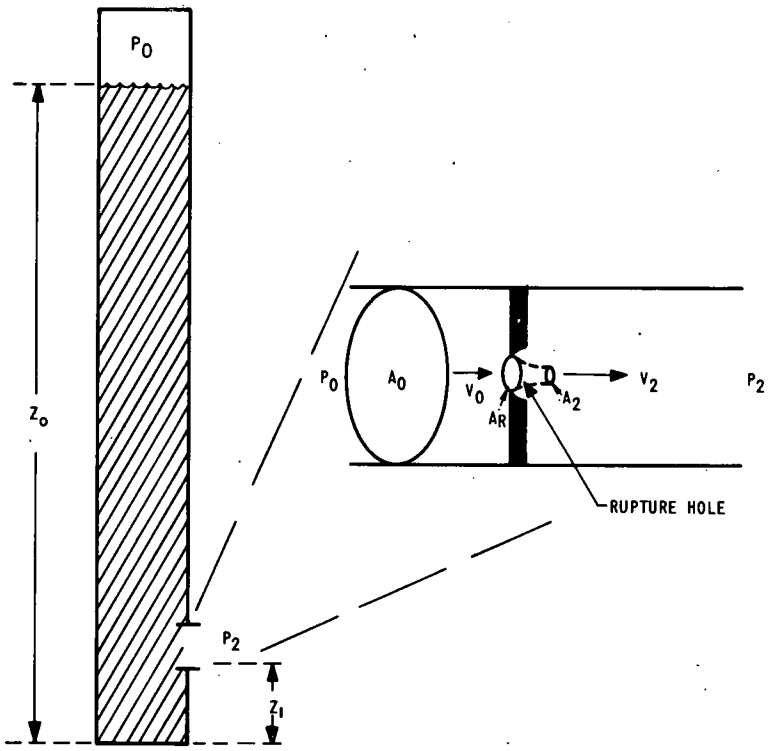

Fig. 49. Model for Sodium-bond Release from a Rupture Hole in Cladding

The weight rate of flow of sodium bond from a rupture hole in lb/sec (F_B) is given by

$$F_B = CA_R \sqrt{\frac{\left[2g_c(P_0 - P_2) + 2g_L\rho_{Na}(Z_0 - Z_1)\right]\rho_{Na}}{1 - \alpha^2}}, \qquad (1)$$

where C is the discharge coefficient;

A_R is the area of the rupture hole, in in.^{2};

g_c is the conversion factor, 32.17 ft-lb/lb(force)-sec^2;

P_0 is the internal fission-gas pressure due to irradiation, in psi;

P_2 is the external system pressure, in psi;

g_L is the local acceleration due to gravity, in ft/sec^2;

ρ_{Na} is the sodium density, in lb/ft^3;

Z_0 is the initial height of sodium bond, in ft;

Z_1 is the distance from bottom of fuel element to rupture hole, in ft;

and

α is the ratio of the cross-sectional area of rupture hole to inside-diameter area of the cladding.

In practice, $2g_L\rho_{Na}(Z_0 - Z_1)$ is very small and is set equal to zero. The factor $1 - \alpha^2$ is set equal to 1.0 since α^2, the square of ratio of the rupture-hole cross section to the inside diameter of the cladding tube, is $<<1.0$ for hole sizes of interest. Therefore, Eq. 1 can be simplified to

$$F_B = CA_R\sqrt{2g_c\rho_{Na}(P_0 - P_2)}. \quad (2)$$

The factor C is the discharge coefficient for the orifice and was varied from 0.5 to 1.0. Figure 50 shows the measured variation of C as a function of Reynolds number A/A_0 for the VDI (Verein Deutscher Ingenieure) standard orifice.[13,14]

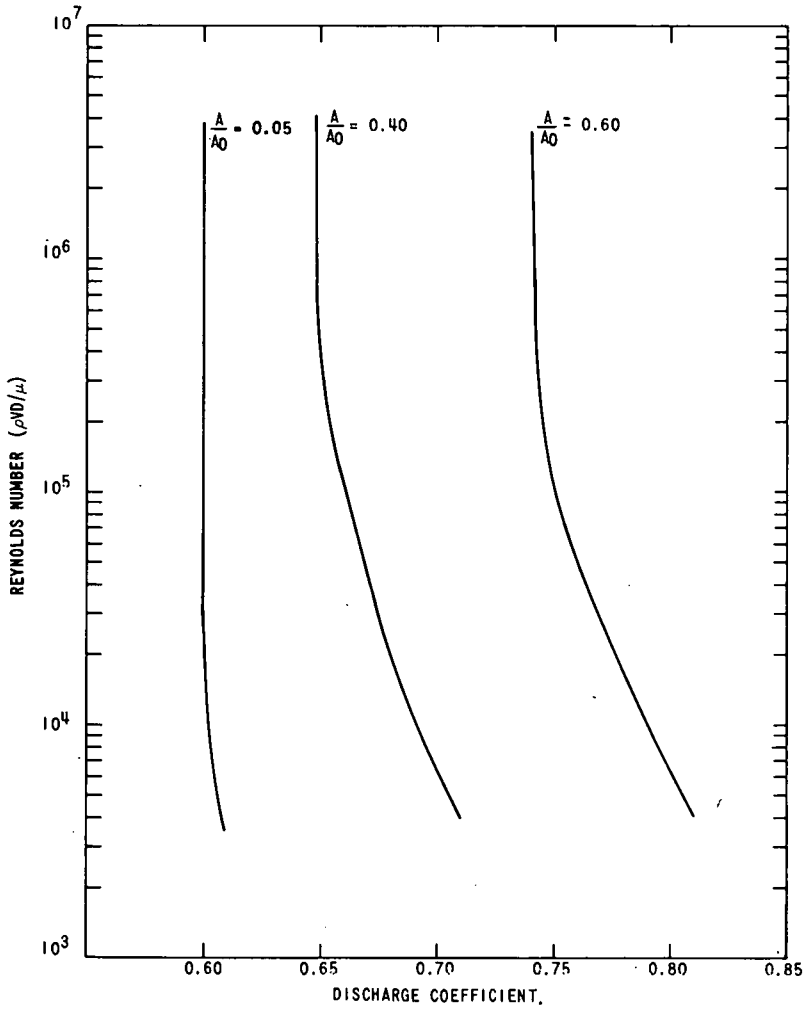

Fig. 50

Discharge Coefficient for a VDI Orifice, as a Function of Reynolds Number and A/A_0

APPENDIX B

Release of Fission Gas

1. Assumptions

The internal fission-gas pressure in a Mark-II fuel element is a function of (a) fission gas released, and (b) fuel swelling. The quantity of gas released from the fuel pin determines a major portion of the internal fission-gas pressure. Fuel swelling in the Mark-II fuel pin is of increasing importance as fuel burnup is increased. The following assumptions were made to bracket the limits of the Mark-II internal fission-gas pressure:

a. All the fission gas produced in the fuel pin is released to the gas plenum. (This case is called "100% released.")

b. The fission gas released is a function of fuel swelling and can be interpreted as given in Fig. 16. (This case is called "experimental data.")

c. The gas-plenum volume is reduced by fuel swelling (i.e., an increase in the sodium-bond level) as follows:

Burnup, MWd/MT	Fraction of Decrease in Gas-plenum Volume
10,000	1.00
20,000	0.90
30,000	0.67
40,000	0.67
50,000	0.67

(This case is called "fuel effect.")

2. Gas Production

Bromine, iodine, krypton, and xenon are assumed to be the only volatile fission products at ≈1000°F.[12] Table IV lists the assumed yields of these gases per 100 fissions[15,16] in the fuel.

The volume (at standard temperature and pressure) of fission gas generated as a function of total energy produced in a Mark-II fuel pin is given by

$$V_{STP} \approx \frac{\frac{\text{atoms}}{\text{fission}} \times \frac{\text{fissions}}{\text{MWd}} \times \frac{\text{liters}}{\text{mole}} \times \frac{\text{cm}^3}{\text{liter}}}{\frac{\text{atoms}}{\text{mole}} \times \frac{\text{cm}^3}{\text{ft}^3}} \qquad (3)$$

or

$$V_{STP} \text{ (for Mark-II fuel pin)} = 0.956 \times 10^{-3} \text{ ft}^3 \text{ per MWd of energy.} \quad (4)$$

The weight of fission-product gases produced can be computed by using the perfect-gas law and assuming the gas produced to be xenon. For the Mark-II fuel pin the weight of gas is calculated as

$$W_{FP} = 3.48 \times 10^{-4} \text{ lb per MWd of energy.} \quad (5)$$

Correcting for the amount of fissionable metal fuel in the fuel pin, we can compute the burnup (B/U) in units of 10,000 MWd/MT per pin and for the Mark-II fuel pin. This quantity is equal to

$$B/U \text{ per pin} = 0.518 \text{ units (of 10,000 MWd/MT).} \quad (6)$$

Therefore, the weight of fission-gas generated may be rewritten so that

$$W_{FP} \text{ per pin} \approx 1.806 \times 10^{-4} \text{ lb (per unit of 10,000 MWD/MT).} \quad (7)$$

TABLE IV. Assumed Yields of Fission-product Gases

Atomic Weight	Stable Gas	Atoms of Gas per 100 Atoms Fissioned							Remarks
		Fast					Thermal		
		^{235}U	^{238}U	^{239}Pu	^{240}Pu	^{241}Pu	^{235}U	^{239}Pu	
79	Br	0.042	-	-	-	-	-	-	Precursor has 6×10^4 years half-life
80	Kr	0.075	0.22	-	0.22	-	1×10^{-5}	0.017	
81	Br	0.135	0.35	-	0.35	-	0.14	0.01	
82	Kr	0.25	0.50	0.008	0.50	0.008	4×10^{-5}	0.02	
83	Kr	0.38	0.64	0.1	0.64	0.1	0.544	0.29	
84	Kr	0.62	0.85	0.2	0.85	0.2	1.00	0.47	
85	Kr	1.15	1.10	0.33	1.10	0.33	0.29	0.127	Gas has 10.6 years half-life
86	Kr	1.65	1.38	0.53	1.38	0.53	2.02	0.76	
87-126	-	-	-	-	-	-	-	-	
127	I	0.26	0.12	0.6	0.12	0.6	0.13	0.39	
128	-	-	-	-	-	-	-	-	
129	I-Xe	0.79	1.00	1.8	1.00	1.8	0.80	1.9	Iodine has 10^7 years half-life
130	-	-	-	-	-	-	-	-	
131	I-Xe	3.2	3.2	4.9	3.2	4.9	2.93	3.78	Iodine has 8 days half-life
132	Xe	4.45	4.7	5.7	4.7	5.7	4.38	5.26	
133	-	-	-	-	-	-	-	-	
134	Xe	7.8	6.6	6.5	6.6	6.5	8.06	7.47	
135	-	-	-	-	-	-	-	-	
136	Xe	6.2	5.9	6.7	5.9	6.7	6.46	6.63	
Totals		27.00	26.56	27.37	26.56	27.37	26.76	27.12	

3. Flow of Fission Gas from a Rupture Hole in Cladding

Figure 51 depicts the model[17] used to simulate fission-gas flow. The rupture hole was treated as a flow nozzle.

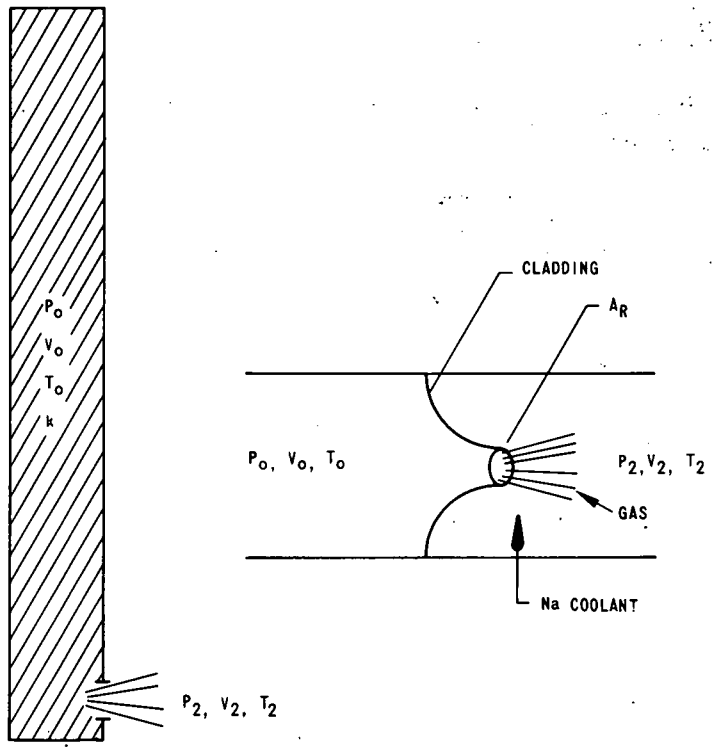

Fig. 51. Model of Fission-gas Release from a Rupture Hole in Cladding

The release of fission gas from the rupture hole will increase as the absolute pressure ratio P_1/P_2 is decreased, until the linear velocity in the nozzle attains the velocity of sound under system conditions. (P_1 is transient pressure, in psi; and P_2 is external system pressure, in psi.) (In this study, system conditions were assumed to be 1000°F and 50 psia.) The value of the pressure ratio at which sonic velocity is achieved (termed the critical pressure ratio, P_{cr}) is given by

$$P_{cr} = P_1/P_2 = \left(\frac{k+1}{2}\right)^{(k/k-1)}, \qquad (8)$$

where $k = C_p/C_v$ is the ratio of specific heats. Values assumed for the specific heats of xenon are

$$C_p = 4.97$$

and

$$C_v = 2.98$$

as predicted by the kinetic theory of gases, so that $k = 1.67$. With this value of k, the critical pressure ratio for fission gas xenon is

$$P_{cr} = P_1/P_2 = 2.05. \tag{9}$$

Under critical-flow conditions, the weight rate of flow of fission gas (ω), in lb/sec, is given by

$$\omega = CA_R \sqrt{\frac{g_c k}{R}\left(\frac{2}{k+1}\right)^{(k+1/k-1)}} \cdot \frac{AP_1}{\sqrt{T_1}}, \tag{10}$$

where R is the universal gas constant; A is cross-sectional area, in in.^{2}; and T_1 is transient temperature, in °F.

A value of 1.00 was used for C, the discharge coefficient, so that

$$\omega = 2.02A_R \frac{P_1}{\sqrt{T_1}}. \tag{11}$$

The total amount of fission gas released at acoustic velocity can be calculated by equating the loss of fission gas from the fuel pin to the total flow through the rupture hole, or

$$-\int_{m_0}^{(m_1)_c} dm_1 = \int_0^{t_c} \omega \, dt, \tag{12}$$

where $(m_1)_c$ is the mass of fission gas at critical pressure ratio for sonic flow, in lb; m_0 is the initial gas mass, in lb; m_1 is the transient mass of fission gas, in lb; and t_c is the time at critical gas flow, in sec.

Substituting Eq. 11 into Eq. 12, we have

$$-\int_{m_0}^{(m_1)_c} dm_1 \approx \int_0^{t_c} 2.02 \frac{A_R P_1}{\sqrt{T_1}} \, dt. \tag{13}$$

Assuming isothermal expansion of the fission gas inside the fuel element, we have

$$\frac{P_1 V_1}{m_1 T_1} \approx \frac{P_0 V_0}{m_0 T_0}, \tag{14}$$

or, since $T_1 = T_0$ and $V_1 = V_0$, we have

$$P_1 = (m_1/m_0)P_0. \tag{15}$$

Substituting Eq. 15 into Eq. 13, and using T_0 for T_1, we have

$$-\int_{m_0}^{(m_1)_c} \frac{dm_1}{m_1} = \int_0^{t_c} 2.02 \frac{A_R P_0}{m_0\sqrt{T_0}}\, dt, \tag{16}$$

and integrating, we have

$$-\frac{1}{2.02} \ln \frac{(m_1)_c}{m_0} = \frac{P_0}{m_0\sqrt{T_0}} A_R t_c \tag{17}$$

or

$$A_R t_c = \frac{m_0\sqrt{T_0}}{2.02P_0}\left[-\ln \frac{(m_1)_c}{m_0}\right]. \tag{18}$$

Thus, if we assume a rupture-hole area (A_R), we can compute the time t_c during which flow of fission gas is at acoustic velocity.

4. Conditions for Fault Propagation

Initial fault-propagation conditions would exist if the adjacent interstitial coolant areas between fuel elements were gas-blanketed (as shown in Fig. 52).

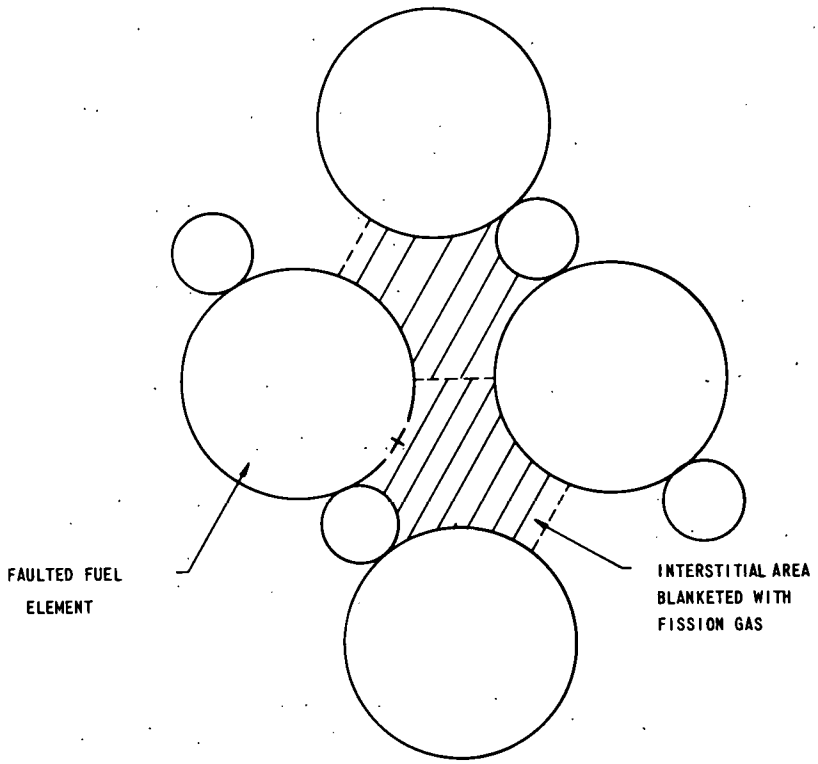

Fig. 52. Fission-gas Blanketing of Interstitial Coolant-flow Area by Cladding Rupture and Gas Release

If EBR-II average system conditions of 30 psi and 1000°F are assumed in the region of the core coolant, the volume in in.^{3} of gas available is given by

$$V_C = \frac{m_2 R T_2}{P_2}, \tag{19}$$

where m_2 is the total mass of fission gas released, in lb. Assuming the local coolant-flow velocity of v_f in./sec and an interstitial flow area of A_f in.^{3}, then a gas discharge rate D.R. of

$$\text{D.R.} = v_f A_f \text{ in.}^3/\text{sec} \tag{20}$$

would keep the local coolant channel around adjacent fuel elements blocked with fission gas.

Since V_C is the volume of gas available, and D.R. the required discharge rate for blockage, the time t_B (in sec) a channel is blocked is given by

$$t_B = \frac{V_C}{\text{D.R.}}. \tag{21}$$

5. Limitations of Fission-gas Model

The above fission-gas fault simulation has the following limitations:

a. The scatter in the fission-gas-release data for Mark-II fuel elements introduces an uncertainty in calculations of gas pressure.

b. The amount of sodium absorbed by Mark-II fuel in the swelling process leads to an uncertainty in the gas-plenum volume.

c. The type of credible rupture that may occur in irradiated material is unknown.

d. The size of credible rupture cracks is unknown.

e. The geometry of credible rupture cracks is uncertain.

f. The effect of turbulent coolant flow on gas discharge was not considered.

g. The influence of wire-wrap supports on gas flow was not considered.

Even with the above-mentioned limitations, however, the models in Section III.A established a plausible upper limit (worst case) for fission-gas blanketing around Mark-II fuel elements.

APPENDIX C

Interactions of Sodium and Molten Fuel

With loss of sodium bond, sodium and molten fuel could interact as a result of uncovering the Mark-II fuel pin. The extent and consequences of this interaction depend on the temperatures of the fuel and bond, the amount of materials involved, and many other system parameters. Because of the complex nature of this problem, only upper-limit calculations were attempted. The following models are based on work by Hicks and Menzies[5] and some later work. The method used in these calculations is based on the following assumptions:

1. The temperature of the molten fuel is above the boiling point of the sodium bond.
2. Sodium and molten fuel are intimately mixed at constant volume.
3. Thermal equilibrium in the mixture is achieved before expansion.
4. Thermodynamic equilibrium is assumed throughout the adiabatic expansion process.
5. After expansion, the pressure of the sodium vapor is down to 1 atm rather than at local system pressure.
6. The liquid fuel and sodium bond are incompressible.
7. The liquid fuel and sodium have negligible specific volume compared with the vapor phase.
8. Sodium vapor behaves as a perfect gas.
9. The specific and latent heats are independent of temperature.

Within the above assumptions, the adiabatic relation for the mixture of molten fuel and sodium is given by

$$(mS_\ell + S_f)\frac{dT}{T} + Ld\left(\frac{x}{T}\right) = 0. \qquad (22)$$

where

m is the mass of liquid sodium, in g/g of fuel;

S_ℓ is the specific heat of liquid sodium, in J/g-°C;

S_f is the specific heat of liquid fuel, in J/g-°C;

T is absolute temperature, in °K;

L is the latent heat of evaporation of sodium, in J/g;

and

x is the mass of sodium vapor, in g/g of fuel.

Integrating this equation, we have

$$\frac{Lx}{T} = (mS_\ell + S_f) \ln T_m/T, \tag{23}$$

where

$$T_m = \frac{mS_\ell T_c + S_f T_f}{mS_\ell + S_f} \tag{24}$$

in which equation T_c is the temperature of liquid sodium, in °K; and T_f is the temperature of liquid fuel, in °K.

The work done in joules (W) during adiabatic expansion is given by

$$W = (mS_\ell + S_f)(T_m - T) - x(L - RT) \tag{25}$$

down to x = m at $T = T_V$ (when the sodium is vaporized), where R is the universal gas constant. The subsequent adiabatic expansion is given by

$$mR \ln [P_V T_V/P] = (mS_{gp} + S_f) \ln (T_V/T) \tag{26}$$

and the additional work by

$$W - W_1 = (mS_{gv} + S_f)(T_V - T). \tag{27}$$

In Eqs. 26 and 27,

P_V is the vapor pressure of the sodium, in dynes/cm^2;

T_V is the temperature at which all available sodium is vaporized in °K;

S_{gp} is the specific heat of sodium at constant-pressure, in J/g-°C;

W_1 is the additional work, in J/g of fuel;

and

S_{gv} is the specific heat of sodium vapor at constant volume, in J/g-°C.

The basic parametric values used in the main body of this report are:

T_f = Variable	T_c = Variable
S_f = 0.16 J/g-°C	S_ℓ = 1.2 J/g-°C
S_{gp} = 0.9 J/g-°C	R = 1/3 J/g-°C
L = 4000 J/g	S_{gv} = 0.005 J/g-°C

Pressure vs temperature (sodium vapor) = log P (atm) = $4.521 - \frac{5220}{T, °K}$

APPENDIX D

Structural Analysis

An energy release from an interaction of sodium and molten fuel could damage the internal structure of a Mark-II fuel subassembly. Analyses of such structural damage are subject to considerable uncertainty resulting from the time dependence of the energy release, the detailed modeling of the geometry of structure, etc. An effort was made to eliminate or at least minimize this uncertainty by establishing upper-limit worst-case conditions. A simple and direct method similar to that of the containment study in the FARET design report was used.[11] This method used the following assumptions:

1. The total amount of energy released radially is one-third the total energy release.

2. The energy is absorbed by plastic stretching of the subassembly structures.

3. Credit can be taken for rapid dynamic loading (i.e., dynamic tensile yield strength is 25% higher than static yield strength).

4. The structural members of a Mark-II fuel subassembly are capable of a total strain of ~0.05.

5. The only structural components considered for energy absorption are (a) the stainless steel members of the subassembly and (b) the fuel pin. No credit is taken for dynamic damping by the sodium coolant.

The total energy release from an interaction of sodium and molten fuel is computed in terms of joules/gram of fuel involved, so that the energy release in inch-pounds is given by

$$E_T = W_T\ (J/g)\ \text{mass}\ (g) \times 4.185\ (\text{cal}/J) \times 3.087\ (\text{ft-lb}/\text{cal}) \times 12\ (\text{in.}/\text{ft}), \tag{28}$$

and the radial damage component of the energy release (in inch-pounds) is

$$E_{RE} = (1/3)E_T. \tag{29}$$

The dynamic tensile-yield strength σ_d (in psi) of Type 304 stainless steel is assumed to be 25% higher than the static tensile-yield strength. In addition, the total strain ϵ_p is assumed to approach 0.05, so that the specific plastic energy E_p is given in in.-lb/in.^{3} by

$$E_p = \sigma_d \epsilon_p, \tag{30}$$

or, for Type 304 stainless steel having a specific weight of 0.283 lb/in.^{3},

$$E_p^{ss} = \frac{\sigma d\epsilon p}{0.283} \text{ in.-lb/lb.} \tag{31}$$

In establishing an upper limit for damage propagation, we have neglected the elastic energy absorption of the Type 304 stainless steel, so that the total amount of steel, in lb, required to attenuate the energy release is given by

$$W_{ss} = \frac{E_{RE}}{E_p^{ss}}. \tag{32}$$

REFERENCES

1. M. H. Shackelford, Ed., *EBR-II Mark-II Driver Fuel Design Report*, March 15, 1968 (Project Report).
2. C. E. Dickerman, L. E. Robinson, F. L. Willis, W. Stephany, and C. August, "Status of Recent Meltdown Studies," *Proceedings of the Conference on Safety, Fuels, and Core Design in Large Fast Power Reactors, October 11-14, 1965*, ANL-7120, pp. 534-539.
3. D. F. Haasl, "Advanced Concepts in Fault Tree Analysis," *System Safety Symposium*, sponsored by University of Washington and the Boeing Company, June 8-9, 1965, Seattle, Washington.
4. C. E. Lapple *et al.*, "Fluid and Particle Mechanics," University of Delaware, Newark, Delaware (March 1956).
5. E. P. Hicks and D. C. Menzies, "Theoretical Studies on the Fast Reactor Maximum Accident," *Proceedings of the Conference on Safety, Fuels, and Core Design in Large Fast Power Reactors, October 11-14, 1965*, ANL-7120, pp. 654-670.
6. H. Savage and R. D. Seibel, *Heat Capacity Studies of Uranium-Fissium Alloys*, ANL-6702 (Sept 1963).
7. S. T. Zegler and M. V. Nevitt, *Structures and Properties of Uranium-Fissium Alloys*, ANL-6116 (July 1961).
8. G. L. Stephens and D. J. Campbell, *Three Dimensional Transient Heat Transfer (THTB)*, General Electric, R60FPD647, Evendale, Ohio (April 1961).
9. C. F. Prutton and S. H. Maron, *Fundamental Principles of Physical Chemistry*, McMillan Co. of New York, Revised Edition (1951).
10. G. H. Golden and J. V. Tokar, *Thermophysical Properties of Sodium*, ANL-7323 (Aug 1967).
11. J. D. Geier, ed., *Fast Reactor Test Facility (FARET): Volume II--Summary of Preliminary Safety Analysis*, ANL-7168 (April 1966).
12. M. J. McNelly, *Liquid Metal Fast Breeder Reactor Design Study, 1000 MWe UO_2-PuO_2 Fueled Plant, Volume II*, GEAP-4418, January 1964.
13. *N.A.C.A.: Standards for Discharge Measurements* (translation of German Industrial Standard, 1952), Tech. Mem. 952, Washington (1940).
14. J. C. Hunsaker and B. G. Rightmire, *Engineering Applications of Fluid Mechanics*, McGraw-Hill Book Company, Inc., New York and London, 1947.
15. Seymour Katcoff, *Fission-product Yields from Neutron-induced Fissions*, Nucleonics *18*, No. 11, pp. 201-208 (1960).
16. L. Burris, Jr., and I. G. Dillon, *Estimation of Fission Product Spectra in Discharged Fuel from Fast Reactors*, ANL-5742 (July 1957), Table 2, p. 18.
17. J. J. Thompson, Atomics International, personal communication.